An Intelligent Detection System for Rheumatoid Arthritis (RA) Disease using Image Processing

By

ABDYRAHYM HAJYYEV

FINAL PROJECT REPORT

Submitted to the Electrical & Electronics Engineering Programme
in Partial Fulfillment of the Requirements
for the Degree
Bachelor of Engineering (Hons)
(Electrical & Electronics Engineering)

Universiti Teknologi Petronas
Bandar Seri Iskandar
31750 Tronoh
Perak Darul Ridzuan

CERTIFICATION OF APPROVAL

An Intelligent Detection System for Rheumatoid Arthritis (RA) Disease using Image Processing

by

abdyrahym hajyyev

A project dissertation submitted to the
Electrical & Electronics Engineering Programme
Universiti Teknologi PETRONAS
in partial fulfilment of the requirement for the
Bachelor of Engineering (Hons)
(Electrical & Electronics Engineering)

Approved:

_____

Zazilah Bt. May
Project Supervisor

UNIVERSITI TEKNOLOGI PETRONAS

TRONOH, PERAK

June 2014

CERTIFICATION OF ORIGINALITY

This is to certify that I am responsible for the work submitted in this project, that the original work is my own except as specified in the references and acknowledgements, and that the original work contained herein have not been undertaken or done by unspecified sources or persons.

Abdyrahym Hajyyev

ABSTRACT

Rheumatoid Arthritis (RA) is an autoimmune disease that causes chronic pain, stiffness, redness or loss of function in the joints. Other than early diagnosis, there is yet a cure available for RA. Diseases with similar symptoms such as lupus, osteoarthritis, gout cause difficulty in diagnosing RA. Currently, indirect immunofluorescence (IIF) test performed to identify ANA in Hep-2 cells. Thus, image processing techniques vital to make diagnosis more efficient, accurate and less time-consuming.

For this project standardized staining pattern classifier to be designed by using image processing techniques. Current manual techniques has limited accuracy and time consuming. In IFF procedures, unsuitable microscope to read Hep-2 cell slides, or photo bleaching effect where cells bleached extremely in short period of time are disadvantages. Another downside is test results being subject to change with experts knowledge and years of experience. These factors lead to low accuracy and it becomes a lengthy process due to large number of images. Out of five types of staining patterns nucleolar and centromere share similar visual appearance and the same is true to homogeneous, fine-speckled, coarse-speckled patterns. This is one of the major factors affecting classification accuracy due to results being subjective.

In this research, First and Second Order Statistics Feature Extraction, Mamdani Fuzzy Logic Classification methods utilized to develop automatic detection system for RA with the help of Matlab R2012b, Fuzzy Logic Toolbox, and Image Processing Toolbox. The algorithm tested on the publicly available Mivia Hep-2 Cell image dataset.

Fuzzy logic classified 85 out of 250 images wrongly. It has 66% accuracy. The images obtained from MIVIA dataset has been manually segmented to cell level from the image level. Developing an automated segmentation algorithm might give better results.

ACKNOWLEDGEMENTS

Foremost I would like to express my gratitude to my supervisor Ms. Zazilah Bt. May for her supervision and support from the beginning of my project. Beside my supervisor, I would like to thank my co-supervisor Ms. Josefina Barnachea Janier for her guidance.

My sincere thanks go to Universiti Teknologi PETRONAS for enabling me to do this project where I improved my knowledge in many ways.

TABLE OF CONTENTS

LIST OF FIGURES

LIST OF TABLES

LIST OF ABBREVIATIONS

- ANA Antinuclear autoantibody
- CLBP Completed Local Binary Pattern
- FCM Fuzzy Clustering Method
- GLCM Grey Level Co-occurrence Matrices
- HEp-2 Human epithelial type 2
- IIF Indirect immunofluorescense
- k-NN k-Nearest Neighbor
- LBP Local Binary Pattern
- NHOG Normalized Histogram of Oriented Gradient
- RA Rheumatoid Arthritis
- RGB Red green blue
- ROI Region of Interests
- SURF Speeded-up Robust Features
- SVM Support Vector Machine

This page intentionally left blank

CHAPTER 1

INTRODUCTION

1.1 Background Study

With the technological advancements in the field of medicine, experts are now capable of assessing precisely more and more medical issues, such as heart disease, cancer, asthma, kidney disease, schizophrenia, tuberculosis. Some of these diseases are easily detectable and treatable, while some remain a great mystery. Rheumatoid Arthritis (RA) is another disorder which carries a great deal of importance since it's cure yet to be discovered. 1% of the world population carries RA while women are diagnosed three times more than men [1-3]. It is an autoimmune disease which causes immune system to attack healthy tissues in the body instead of damaged tissues like virus and bacteria. RA is an chronic, progressive disorder that affects many parts of the body. Mainly, a thin membrane between joints and synovium are attacked. The excessive fluid in the joints causes pain and triggers the wreckage of articular cartilage and ankylosis of the joints, inflammation in the lungs. The Figure 1 shows the image of normal joint vs. arthritic joints [4-6].

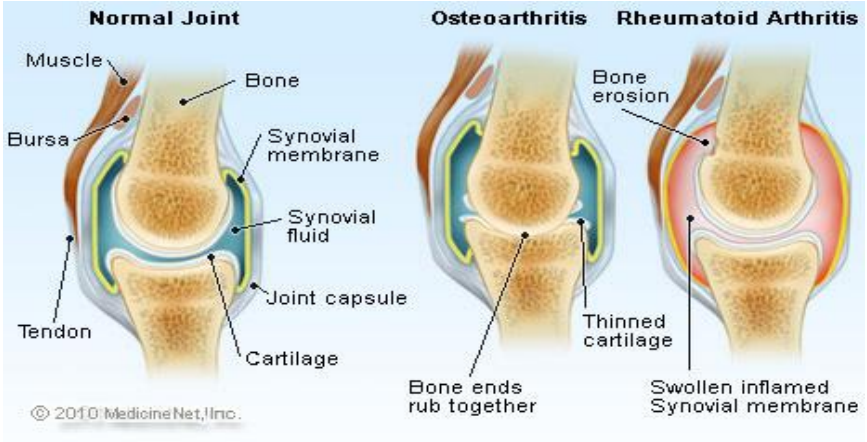

Figure 1: Normal joint vs. Arthritic joints [6]

The inflammation can spread to ligaments, tendons, muscles and RA causes stiffness, redness, swelling in the joints. Due to its peculiar nature, RA has to be diagnosed as soon as possible to avoid long term chronic pain or loss of function in the joints. [6]

Antinuclear Antibodies (ANA) has to be identified in Hep-2 cells to diagnose RA and indirect immunofluorescence (IFF) test used to detect ANA. A sample slide with a Hep-2 cell observed under the fluorescence microscope. IFF test followed with two preceding steps which are observing the fluorescence intensity and classifying patterns [7]. Fluorescence intensity categorized into three levels - positive, negative, intermediate and patterns classified as positive or intermediate class [8]. There are five types of staining patterns and combination of patterns indicate different autoimmune diseases [9].

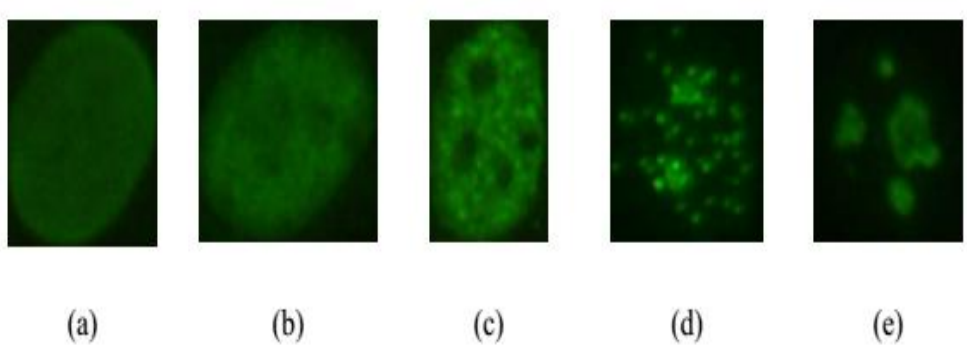

Figure 2: (a) homogeneous (b) fine speckled (c) coarse speckled (d) centromere (e) nucleolar [10]

Pattern	Description
Homogeneous	Diffuse staining, consistent across the whole nucleus
Fine speckled	Fine granular nuclear staining
Coarse speckled	Coarse granular nuclear staining, larger specks
Centromere	Large numbers of strong bright spots on a darker ground
Nucleolar	Large speckled staining with less than six in number within the nucleus

Table 1: Characteristics of staining patterns [9]

From the five types of patterns, fine speckled is present in healthy individuals only, whereas homogeneous, centromeric, coarse specked and nucleolar ANA staining patterns existed in patients with RA [11]. Several segmentation, feature extraction, classification methods will be analyzed to detect RA successfully and the most applicable methods will be implemented and tested in Matlab.

1.2 Problem Statement

In this project standardized staining pattern classifier to be designed by using image processing techniques. Current manual techniques has limited accuracy and time consuming. In IFF procedures unsuitable microscope to read Hep-2 cell slides, or photo bleaching effect where cells bleached extremely in short period of time are disadvantages. Another downside is test results being subject to change with experts knowledge and years of experience. These factors lead to low accuracy and it becomes a lengthy process due to large number of images. Out of five types of staining patterns nucleolar and centromere share similar visual appearance and the same is true to homogeneous, fine-speckled, coarse-speckled patterns. This is one of the major factors affecting classification accuracy due to results being subjective.

1.3 Objectives

1. To study segmentation, feature extraction, classification methods and to choose the most suitable techniques to identify RA by analyzing ANA staining patterns.
2. To validate the accuracy of selected classification technique results.

1.4 Scope of Study

1. Study ANA staining patterns to distinguish RA from other diseases.
2. Familiarize with First-Order Statistics Feature Extraction, Fuzzy Logic Classification.
3. Learn MATLAB R2012b for image processing to develop algorithm for feature extraction, pattern recognition respectively.

1.5 Relevancy of the project

This project is related to image processing where the most suitable and accurate feature extraction, classification methods will be used to detect RA by analyzing ANA staining patterns. The automated system will assist doctors to diagnose RA patients much faster and more accurately.

1.6 Feasibility of the project

The project mainly involves simulation of the developed algorithm to detect ANA in Hep-2 cells from publicly available MIVIA image dataset. The project is economical and time frame of 28 weeks dedicated for FYP I and FYP II is sufficient to complete the project successfully on time.

CHAPTER 2

LITERATURE REVIEW

In Figure 3, the proposed method to classify Hep-2 cells are shown. The cell image which went acquisition process retrieved from the image acquisition unit. The cell image undergoes image segmentation and followed by feature extraction of the image to extract cell information. Extracted cells (Ncells) used as an input to classify cell pattern [12].

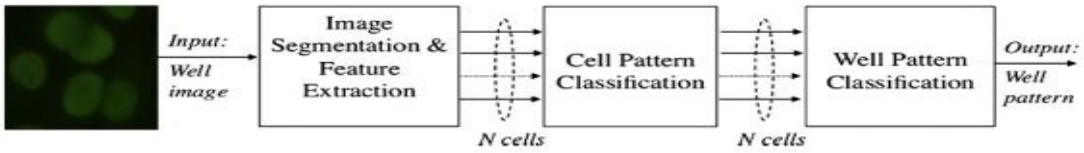

Figure 3: Steps to classify Hep-2 cells [13],[14]

2.1 Mivia Project (Classification of Immunofluorescence Images for the Diagnosis of Autoimmune Diseases) Dataset Description

The dataset obtained from Mivia has 28 images total with images segmented into multiple staining patterns. There are total of 6 pattern distributions which are homogeneous, centromere, coarse-speckled, fine-speckled, nucleolar and cytoplasmic [9]. Image resolution is 1388x1038 with 24 bit color depth. The dataset summary shown in Table 2.

Total images	28
Pattern Distribution	Homogeneous - 5; Centromeric - 6; Coarse Speckled - 5; Fine speckled - 4; Nucleolar - 4; Cytoplasmic - 4
Resolution / Color Depth	1388x1038 pixels / 24 bits
Hep-2 Cell Information	Staining pattern, fluorescence intensity, mitosis phase, seed object coordinates
Hep-2 Dilution	1:80
Storage format	Uncompressed

Table 2: Mivia data description [9]

2.2 Segmentation

The Table 3 summarizes the most common segmentation methods such as Watershed, Otsu's thresholding, Fuzzy Clustering Method (FCM), and Artificial Neural Network (ANN) [13-24].

Method:	Limitations:	Overcome limitations using:	Combined with:
Watershed Segmentation: combination of edge and region based techniques	• Over-segmentation • Sensitive to noise • Poor detection in low contrast contour	• Marker image • Use isotropic filter to reduce noise • Use otsu thresholding as a preliminary technique	• Fast Region Merging - to overcome over-segmented images • Wavelet Transform - to enhance image edge and to eliminate noise before the Watershed segmentation
Otsu's Thresholding: converting the multilevel image into binary image	• Overlapping cells • Suspect to noise • Fails to recognize nucleolar and speckled patterns	• Circulatory measure • Erosion and dilation techniques	• None
Fuzzy Clustering Method (FCM): used to differentiate between foreground and background	• Separated into single cluster • Sensitive to color variation • Long computing time	• Use Fuzzy-C means (FCM)	• None

Artificial Neural Network (ANN): segmentation through linear approximation from finite element simulations	• Complex computation • Requires extensive training data	• Genetic Algorithm (GA) applied to SOM output	• None

Table 3: Segmentation Methods [13-24]

Image segmentation is a vital step in the automated detection system of ANA in Hep-2 cells. Segmentation involves diving the image into multiple Regions of Interests (ROI) according to predetermined parameters such as color, texture, intensity. In segmentation images decoded into pixels to improve the shape and the edge of an object. Image segmentation is reliable and crucial part of medical imaging where each image differ one from another in terms of color intensity, dimension, texture. It preserves the originality of an image shape, texture while reducing image noise and blur [23], [25]. In Figure 4, over-segmentation of watershed method shown and in Figure 5 depicts the use of Fast-Region merging technique to overcome over-segmented images.

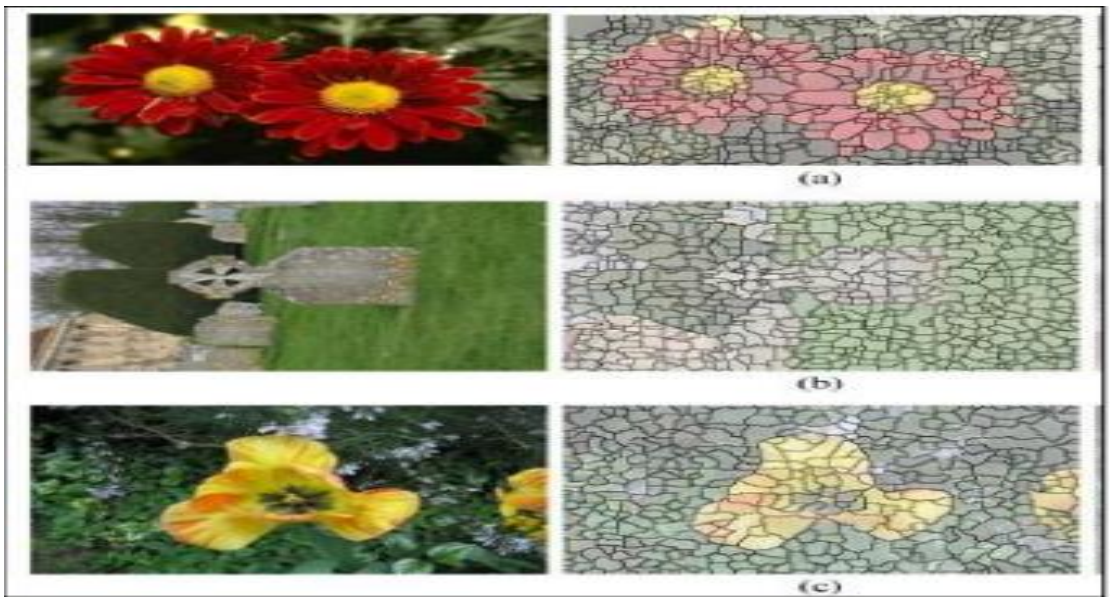

Figure 4: Over-segmentation of Watershed method [25]

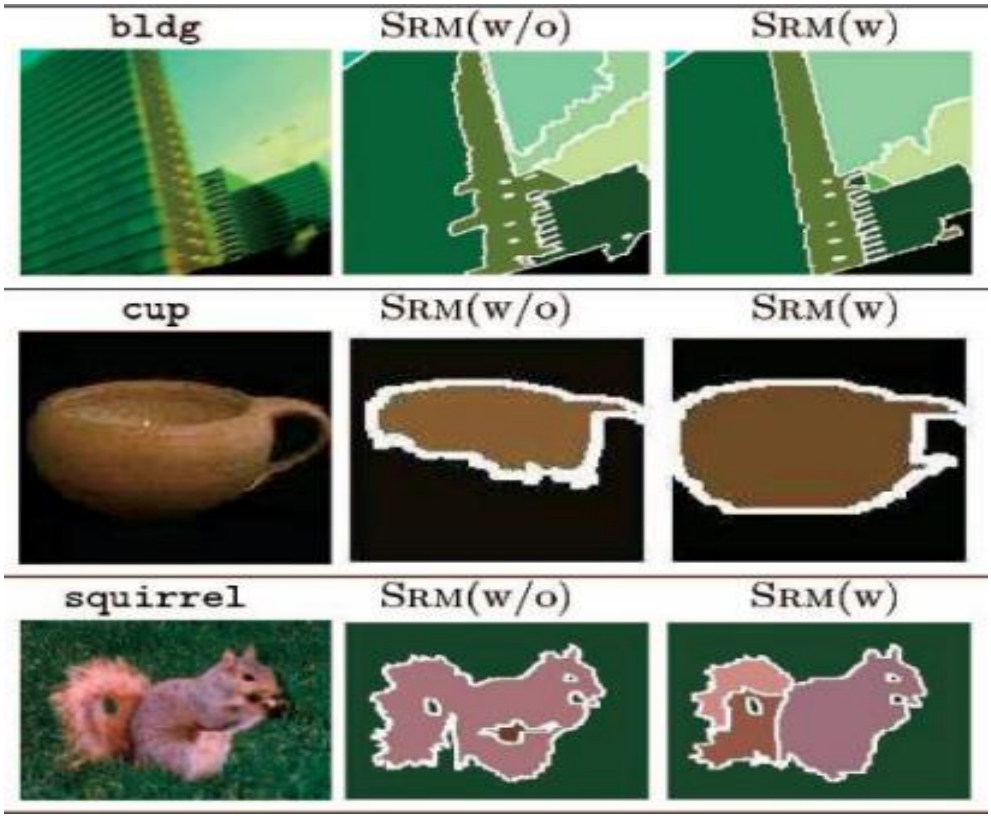

Figure 5: Fast Region Merging Technique to overcome over-segmented images [23]

Analysis on Segmentation Literature Review

Segmentation is a key component to detect ANA in Hep-2 cells and each method bears different limitations, advantages. Otsu's thresholding produces good outcome and easy to operate. However, it fails to recognize nucleolar, speckled patterns. FCM's sensitivity to color variation a major limitation despite its flexibility. ANN segmentation technique requires vast amount of training data which is unavailable in the publicly available Mivia dataset. Watershed segmentation is a reliable method with simple algorithm and promising results. Watershed drawbacks can be eliminated by combining with Fast Region Merging to overcome over-segmentation and Wavelet Transform to reduce noise, to enhance image edge. Thus, Watershed segmentation is the most suitable method to detect ANA in Hep-2 cells. However, MIVIA provides images are already been segmented.

2.3 Feature Extraction

Features like correlation, homogeneity, energy, contrast, entropy will be extracted. There are many feature extraction methods. Different research papers analyzed on these methods and their suitability for this project. The Table 4 shows accuracy percentages for Histogram of Gradient (HOG), Textural - Grey Level Co-occurrence Matrix (GLCM), Region of Interest (ROI), and Speeded-Up Robust Features [26-30].

Feature Type	Percentage of Accuracy								
	Intensity-wise		Class-wise						Overall
	Positive	Inter	HO	FS	CS	NU	CY	CE	
HOG	83.84	80.31	82.67	64.89	93.58	70.59	82.76	89.42	82.25
Texture	90.40	81.54	87.33	68.09	96.33	86.27	68.97	93.75	86.39
ROI	80.56	50.78	87.33	0	88.99	58.82	86.21	70.19	67.13
SURF	77.53	57.85	68.67	44.68	59.63	76.47	84.48	75.96	68.67

Table 4: Percentage accuracy of feature extraction methods [26-30]

In Table 5 feature extraction methods Completed Local Binary Pattern (CLBP), 2D Gabor Filter, Standard Local Binary Pattern (SLBP) analyzed and compared one with another [31-33].

AUTHORS	S.Singh, R.Maurya, and A.Mittal	A.Tahmasebi, H.Pourghassem and H. Mahdavi	O.Lahdenoja , M.Laiho, A.Passion
YEAR	2012	2011	2005
FEATURE EXTRACTION	Completed Local Binary Pattern (CLBP)	2D Gabor Filter	Standard Local Binary Pattern
ADVANTAGES	- One of most powerful texture descriptor among LBP variants. - Simple and efficient operator. - Outperform other feature extractor method - Low cost discriminative characteristics for facial recognition system	- Able to extract feature such as spatial locality , orientation selectivity and also some distinct features	- Standard LBP variants - Invariant with respect to monotonic gray-scale. - Outperform all the state of the art such as PCA, LDA and EBGM. - Can be extracted faster in a single scan compared to Gabor wavelets.
RESULT	- Average of the accuracy is higher compared to the other method. - Achieves accuracy of 86.4% when used with Multi Class Support Vector Machine (MCSVM) - Higher accuracy compared to the standard LBP.	- Combination of this technique with k-NN classifier produces a robust fusion technique for ear identification system. - Proposed method needed more processing time as Gabor Filter will produce a large dimension of the filtered image.	- Shows the highest accuracy for four different classes with the average accuracy of 70.8%.
APPLICATION	- Facial expression recognition - Dynamic texture recognition - Shape localization	- Ear identification system	- Industrial wood - Paper inspection - Motion detection - Face recognition

Table 5: Summary of Feature Extraction Methods [31-33]

The Table 6 summarizes statistical feature extraction methods [34-36].

Author	Technique	Applications	Advantages	Disadvantages
G. Srinivasan and G. Shobha [18]	First order statistics	Obtained from original image values	Easy to analyse characteristics of image from histogram	Does not provide information on relative position of pixels to each other
	Spatial frequencies	Define texture by the number and types of primitives	Able to characterize texture as fine or coarse based on tone and structure characteristics of the primitives	Same number, type of basic patterns and spatial relationship does not imply same texture
	Law's texture energy measures	Determine texture properties by assessing average grey level, edges, spots, ripples and waves	Derive 5 texture properties from three simple vectors	Long computation
A. Materka and M. Strzelecki [19]	GLCM	Estimate image properties by taking into account relationship between pixels or group of pixels	• Consider spatial properties • Simple	Does not consider primitive shape
	Fractal-based	Provides a description on the complexity or irregularity of an object	High relation with human judgement to surface roughness	Uniform in all orientations
R. Maini and H. Aggarwal [20]	Edge frequency	Measures the total length of all edges in a region to measure coarseness or complexity of a texture	Usage of simple operators such as Robert's and Sobel's to analyse textures	Depends on the size of object and sensitive to noise

Table 6: Feature extraction statistical methods [34-36]

Analysis on Feature Extraction Literature Review

There are number of feature extraction methods. Statistical, Textural, CLBP, GLCM methods perform better in comparison to the rest of the methods. The combination of First-Order and Second-Order statistics is powerful to distinguish Hep-2 images.

2.4 Classification

The Table 7 below summarizes classification methods [37-42].

Method:	Classification Principle:	Advantages:	Limitations:
Support Vector Machine (SVM)	Based on the concept of decision planes and separates the classes by creating	- Simple algorithm - High accuracy	- Binary classifier, differentiates between two groups only.

	a clear boundaries between them		
Maximum-Likelihood Classification (MLC)	Estimate parameters of a statistical model in which a data set is applied. MLC will estimate mean and variance of the tested image according to the determined value beforehand.	- Good RGB image classifier	- Low accuracy - Unable to classify low intensity images
Fuzzy Logic Classification	Aims to model the human reasoning and applying the model to problems. Mamdani and Sugeno are two types of fuzzy logic system where Mamdani expects the output membership functions to be fuzzy sets and requires defuzzification.	- Able to classify low intensity images - Tolerant to inexact data - Able to model complex nonlinear functions - Easy to understand due to linguistic form - Easily maps the input parameters to output parameters	- Requires fine tuning and simulation before it can be operational
k-Nearest Neighbor (k-NN)	Works by memorizing the whole training data and performs classification if the attribute test object matches one of the training examples exactly where ‘k’, is the number of nearest neighbors and this chosen to optimize the result of classification	- Simple algorithm - High accuracy - High sensitivity and high specificity - Able to recognize most of the ANA patterns	- Difficulty to recognize mixed patterns

Table 7: Classification Method Summary [37-42]

Classification is the final step in Image Signal Processing where it is used to differentiate between images. In this project five types of staining patterns need to be classified. There are several classification methods and SVM, k-NN, Fuzzy Logic, MLC are the most popular ones. From the figure above, it is clear that Fuzzy Logic is the most suitable choice. SVM is binary classifier which is unable to classify five different staining patterns. MLC is unable to classify low intensity images and has low accuracy. Some of the staining patterns will be low intensity. Despite its simplicity and high accuracy, k-NN is not suitable for this project because it has difficulty recognizing mixed patterns. Fuzzy logic possesses numerous advantages and the only limitation of its can be overlooked since the algorithm will be tested beforehand. Mamdani-type fuzzy logic is more suitable since it makes the output membership functions to be fuzzy sets and requires defuzzification. Mamdani uses rule-based structure to get desired system output response depending on the system input parameters. The Figure 6 depicts the rule-based structure [37-42].

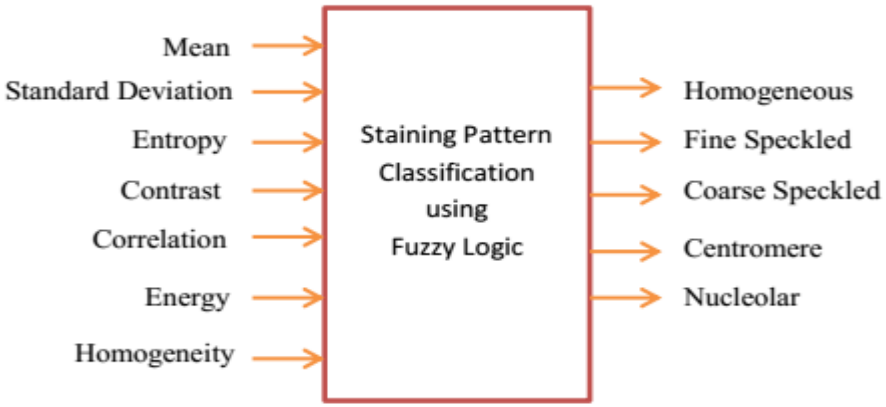

[38]

Figure 6: Rule-based structure [37-42]

2.5 Current RA Detection Tools

❖ X-ray / Radiograph

X-ray or radiograph is widely used to assess the joint damage in RA patient. Hand and wrist radiographs are vital to obtain clinical information. X-rays applied both to monitor the disease progression over time and effects of drugs to overcome RA. The image below shows radiograph of the hand with bone erosion[4, 43].

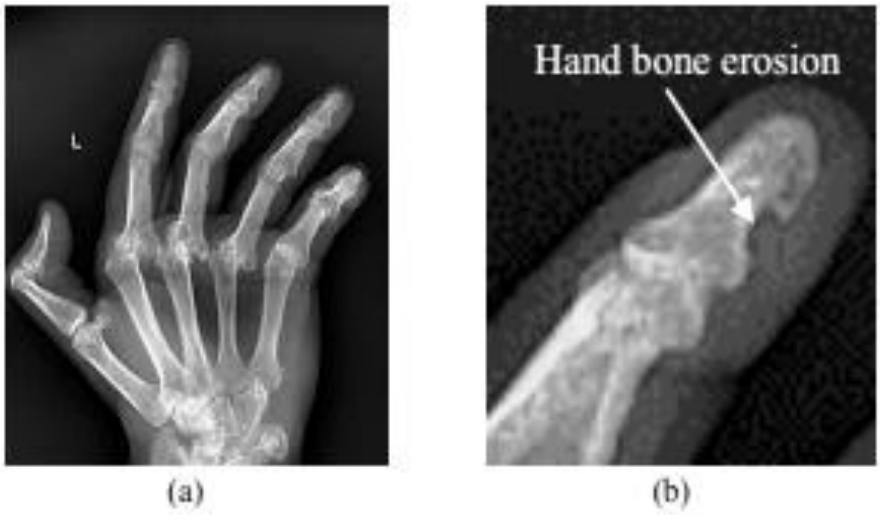

Figure 7: Radiograph of the hand with bone erosion [44]

X-ray shows the time-integrated overall joint damage. Low cost, high availability, centralized reading , good reproducibility and the validated testing techniques are some of the advantages radiographs possess. It is used to seperate RA from similar diseases like osteoarthritis, neoplasm. Radiographs capable of performing bone boundary detection through methods such segmentation and contour. The Level Set Method (LSM)being used for image segmentation but the LSM affected by noise and unclear boundaries causing complete breakdown or early termination of the curve evolution process. There is new modified LSM which makes use of diffusion filter and the results still below expected performance. Further research has to be done[44-45].

❖ **Magnetic Resonance Imaging (MRI)**

MRI is an essential tool to monitor RA progression, bone erosion and effect of drug treatment. It uses segmentation propagation algorithm to identify two separate bones in the ankle of experimental rat model of RA.

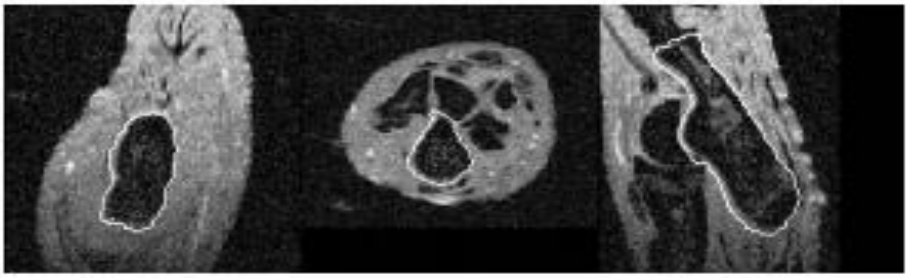

Figure 8: MRI scan on experimental rat [46]

MRI shows that registration algorithm used to determine the volume of bones and distances between them which provides quantitative information on RA progression[46].

❖ **Near Infrared (NIR) Optical Imaging**

NIR is a fast growing electromagnetic spectrum has two major advantages over light in the visible spectrum for imaging. Firstly, NIR light has lower absorption in the biological tissues than visible light which means information from deeper structures can be analyzed. NIR light has lower auto fluorescence compared to visible wavelengths. NIR imaging mainly provides surface weighted reflectance images and reconstruction of light based on diffuse optical properties[47-48].

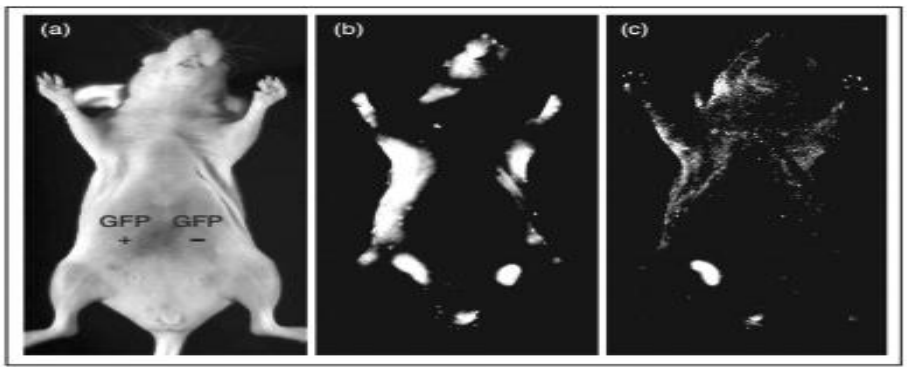

Figure 9: NIR imaging of experimental rat [47]

CHAPTER 3

METHODOLOGY

3.1 Project Activities

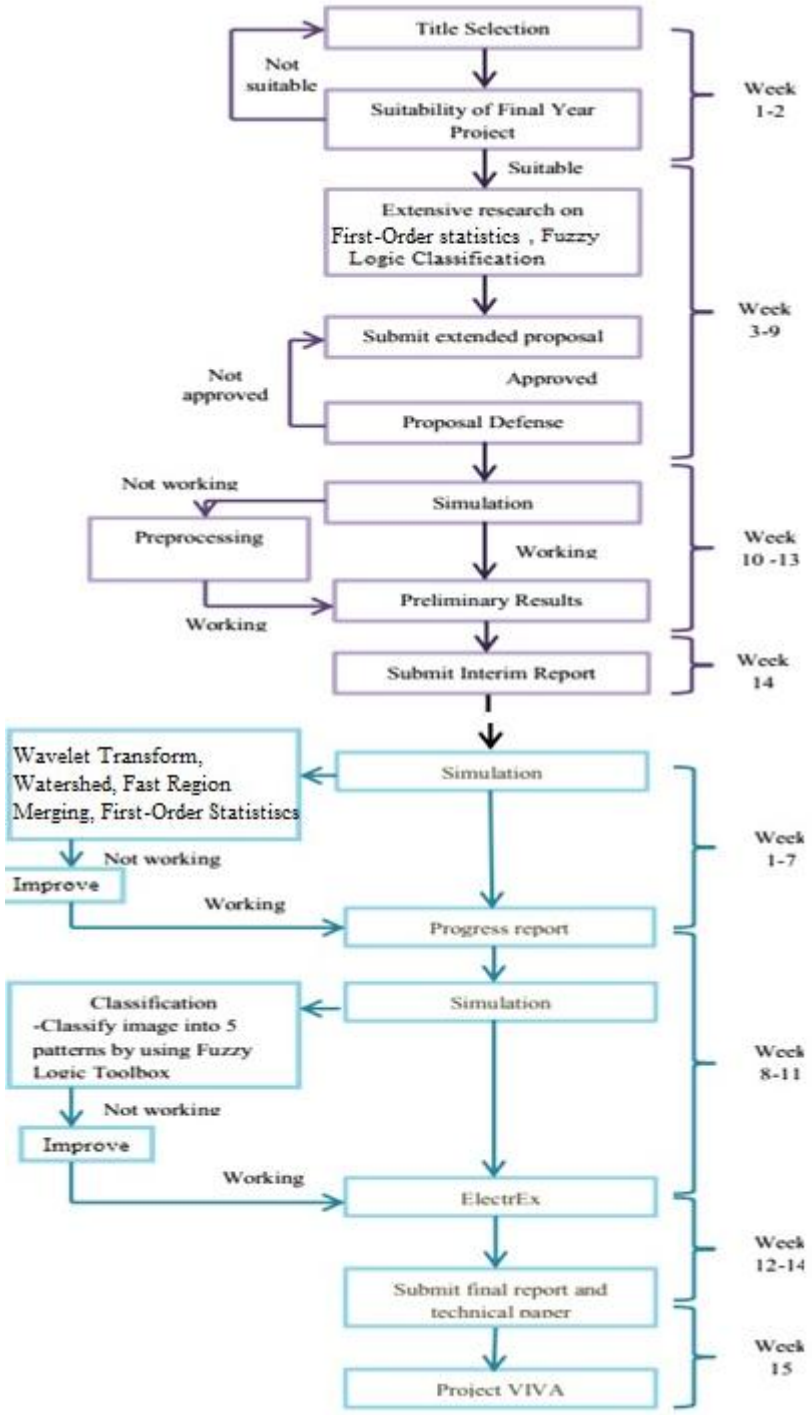

Figure 10: Overall activities for FYP I and future activities for FYP II

3.2 Research Methodology

The Figure 11 illustrates overall image processing flow.

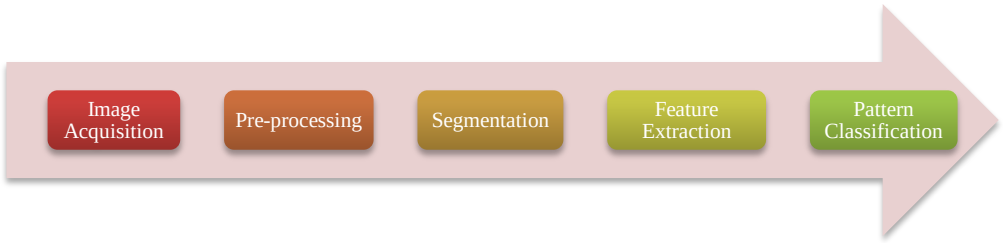

Figure 11: Image Processing Flow

3.2.1 Image Acquistion

Mivia Hep-2 images dataset used for this project and dataset description discussed in Chapter 2.1.

3.2.2 Pre-processing

Wavelet Transform pre-processing used to reduce noise and to enhance image quality such contrast, intensity, brightness.

3.2.3 Feature Extraction

First-Order and Second-Order Statistics used to extract the textural features once the Hep-2 image has been segmented. First-Order calculates properties while ignoring spatial interaction between pixels. Second-Order used to complement this issue. It calculates properties of two pixels when certain location values occur relative to each other and takes different angles, distances of neighboring pixels into consideration [34-36]. Total of seven features will be extracted. They are:

1. Mean - calculated in Matlab by taking the mean values of elements.

2.

$$Standard\ Deviation = \left(\frac{1}{n-1}\sum_{i=1}^{n}(x_i - \bar{x})^2\right)^{\frac{1}{2}}$$

3. Entropy - measure of randomness

$$Entropy = -sum(p \times \log_2 p)$$

4.

$$Contrast = \sum_{i,j}|i-j|^2 p(i,j)$$

5.

$$Correlation = \sum_{i,j}\frac{(i-\mu i)(j-\mu j)p(i,j)}{\sigma_i \sigma_j}$$

6.

$$Energy = \sum_{i,j}p(i,j)^2$$

7.

$$Homogeneity = \sum_{i,j}\frac{p(i,j)}{1+|i-j|}$$

3.2.4 Pattern Classification

Fuzzy Logic Toolbox will be used to classify five staining patterns from seven features extracted.

3.3 Gantt Chart - Key Milestones

The study plan includes both FYP 1 and FYP 2 which is total of 28 weeks. The Gantt Chart included in the appendix A1, whereas desired milestones shown clearly.

3.4 Tools

- Matlab R2012b (Image Processing Toolbox, Fuzzy Logic Toolbox)
- Microsoft Word 2007
- Microsoft Excel 2007

CHAPTER 4

RESULTS AND DISCUSSION

4.1 Pre-processing and Feature Extraction

Hep-2 images obtained from Mivia dataset are converted from RGB to grayscale image where process outcome can be seen in the Figure 12.

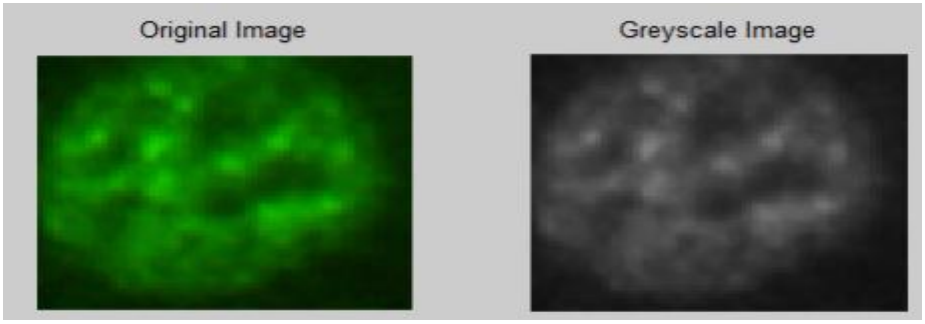

Figure 12: RGB image and Grayscale image

The seven features are extracted from total of 621 training images and 250 testing images. First order statistics, second order statistics and GLCM coding which is shown in Appendix A3 used to extract features which are mean, standard deviation, entropy, contrast, correlation, energy and homogeneity. Once the features extracted in Matlab, seven features exported to Microsoft excel to calculate minimum, maximum and average for each particular staining pattern.

4.2 Classification

Mamdani interface of Fuzzy Logic Toolbox used to classify staining patterns. The extracted seven features acts as an input while the staining patterns are respective outputs. The features extracted are used as an input for the membership functions where each feature will have 5 membership functions from MF1 to MF5. Gaussian membership function used because it is smooth and non-zero at all points. These membership functions will help to calculate the output values which then shown as staining patterns. The shape for the output staining pattern is triangular due to its effectiveness and simplicity. Output parameters values go from 0.2 to 1 with 0.2 interval. Once the output parameters along with membership functions are defined, the rule-based fuzzy logic is set up. From Figure 13 to Figure 18 illustrate the process.

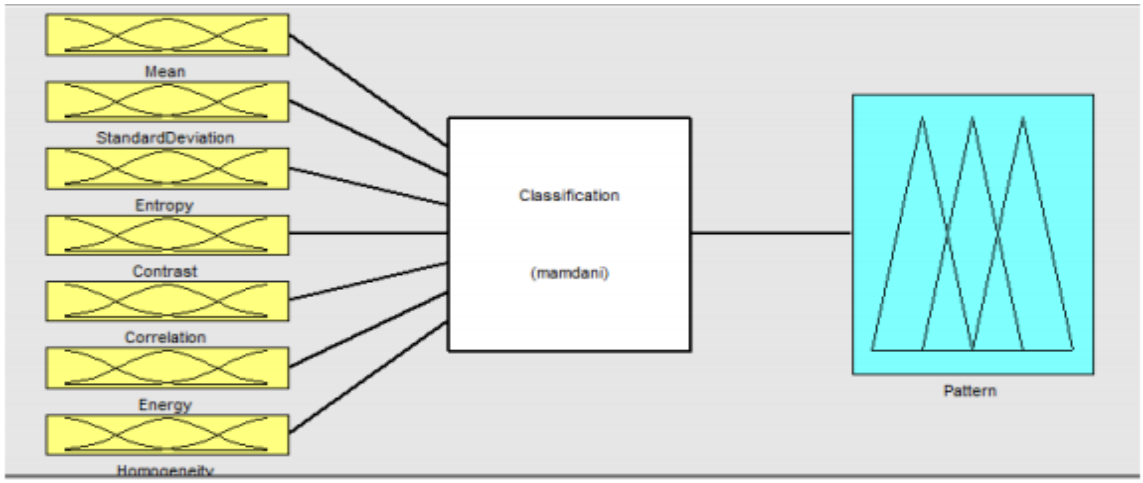

Figure 13: 7 features as an input and output pattern

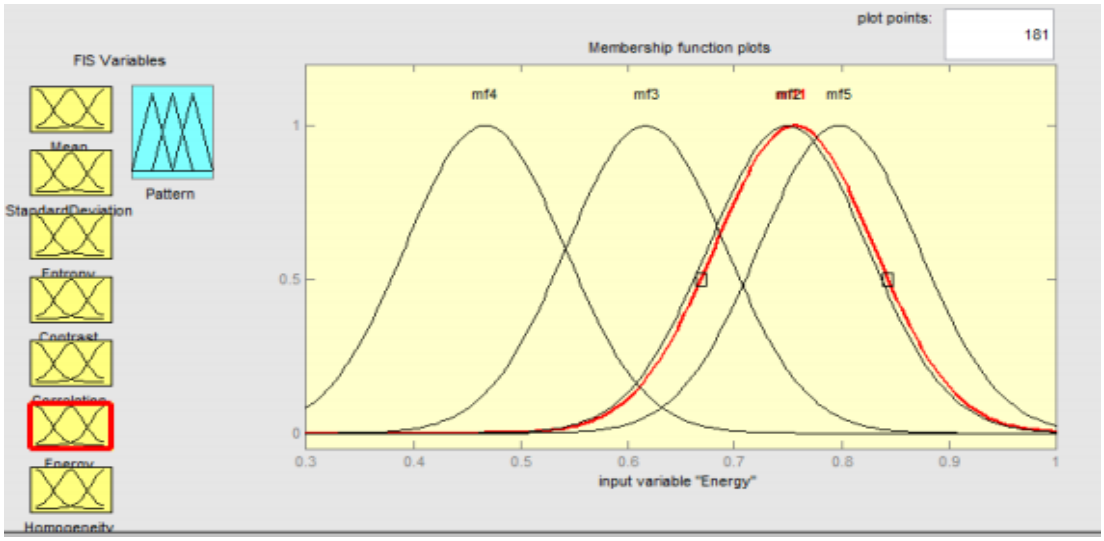

Figure 14: Membership function range for each feature

Pattern	Mean	Standard Deviation	Entropy	Contrast	Correlation	Energy	Homogeneity
Homogenous	mf1	mf1	mf1	mf1	mf1	mf1	mf1
Fine Speckled	mf2	mf2	mf2	mf2	mf2	mf2	mf2
Coarse Speckled	mf3	mf3	mf3	mf3	mf3	mf3	mf3
Centromere	mf4	mf4	mf4	mf4	mf4	mf4	mf4
Nucleolar	mf5	mf5	mf5	mf5	mf5	mf5	mf5

Figure 15: Respective membership functions

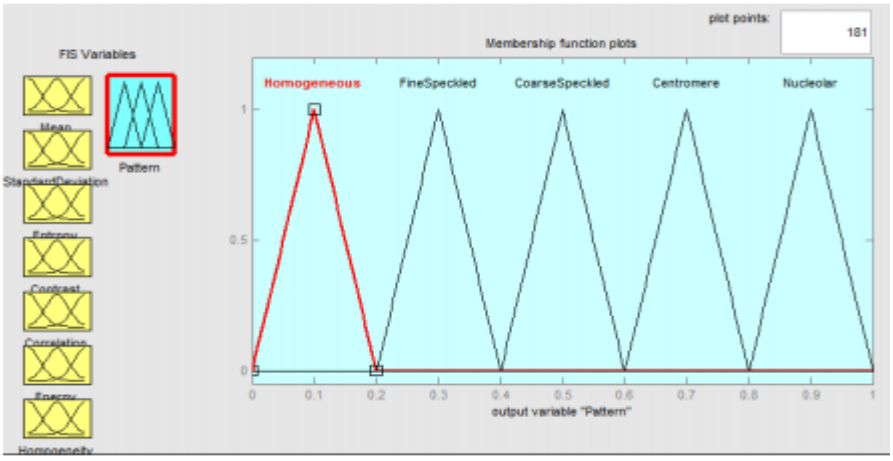

Figure 16: Staining patterns as an output

Patterns	Parameter
Homogenous	0 – 0.2
Fine Speckled	0.201 – 0.4
Coarse Speckled	0.401 – 0.6
Centromere	0.601 – 0.8
Nucleolar	0.801 – 1.0

Figure 17: Parameter values for staining pattern outputs

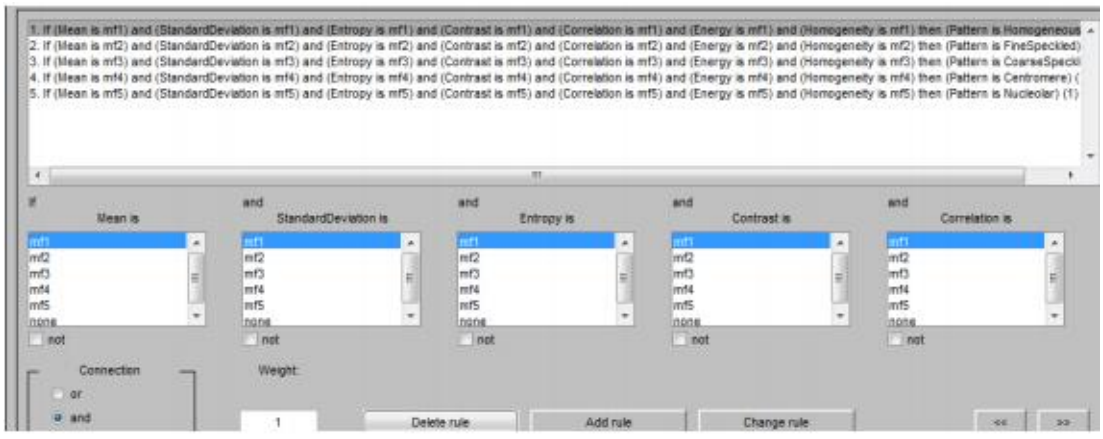

Figure 18: The Rule-based Fuzzy Logic Algorithm

The features extracted from 621 training set and classification results of 250 testing set shown in the Appendix A3 and A4 respectively. The Fuzzy Logic unable to classify correctly 85 images out of 200. Classification has 66% accuracy.

CHAPTER 5

CONCLUSION

The project aims to classify Hep-2 cells according to staining patterns to determine RA disease through ANA test. Each Hep-2 cell image will undergo Wavelet Transform image pre-processing, First-Order statistics feature extraction along with Second-Order Statistics method and Mamdani Fuzzy Logic classification technique. Mean, standard deviation, entropy, contrast, correlation, homogeneity, energy textural features extracted and Mamdani algorithm used these features to perform classification.

Fuzzy logic classified 85 out of 250 images wrongly. It has 66% accuracy. Overall, classification accuracy can be increased further. The images obtained from MIVIA dataset has been manually segmented to cell level from the image level. Developing an automated segmentation algorithm might give better results. As well increasing number of features extracted by using other statistical models such as Law's texture energy measures which determines texture properties by assessing average grey level, edges, spot, ripples, waves will help to increase accuracy. Further experimenting with defuzzification method and membership function type combinations such as triangular, gaussian, trapezoidal membership functions and centroid, bisector and largest of maximum (LOM) defuzzification methods shows it is possible to achieve higher classification accuracy.

REFERENCES

[1] C. Schueller-weidekamm, "Modern ultrasound methods yield stronger arthritis work-up," *Diagnostic Imaging,* vol. 32, 2010.

[2] O. M. R. Westwood, P. N. Nelson, and F. C. Hay, "Rheumatoid factors: what's new?," *Oxford Journals,* vol. 45, pp. 379-385, 2006.

[3] C. Nordqvist. (2010, 2/09/2014). All About Rheumatoid Arthritis. Available: http://www.medicalnewstoday.com/info/rheumatoid-arthritis/rheumatoid-arthritis-diagnosis.php

[4] R. M. Valente, H. S. Luthra, and R. A. Robb, "Quantitative analysis of joint images from patients with rheumatoid arthritis," in *Engineering in Medicine and Biology Society, 1989. Images of the Twenty-First Century., Proceedings of the Annual International Conference of the IEEE Engineering in*, 1989, pp. 1971-1972 vol.6.

[5] H. Simon. (2013, 10 February 2014). Rheumatoid arthritis. Available: http://umm.edu/health/medical/reports/articles/rheumatoid-arthritis

[6] W. C. Shiel Jr. (2013, 2/11). *Rheumatoid Arthritis (RA)*. Available: http://www.medicinenet.com/rheumatoid_arthritis/article.htm

[7] S. Di Cataldo, A. Bottino, E. Ficarra, and E. Macii, "Applying textural features to the classification of HEp-2 cell patterns in IIF images," in Pattern Recognition (ICPR), 2012 21st International Conference on, Tsukuba,Japan, 2012, pp. 3349-3352.

[8] G. Iannello, L. Onofri, and P. Soda, "A bag of visual words approach for centromere and cytoplasmic staining pattern classification on HEp-2 images," in ComputerBased Medical Systems (CBMS), 2012 25th International Symposium on, Rome,Italy, 2012, pp. 1-6.

[9] MIVIA HEp-2 Images Dataset, 2010. [Online].Available: http://mivia.unisa.it/datasets/biomedical-image-datasets/hep-2-image-dataset/

[10] V. Snell, W. Christmas, and J. Kittler, "Texture and shape in fluorescence pattern identification for auto-immune disease diagnosis," in Pattern Recognition (ICPR), 2012 21st International Conference on, Tsukuba,Japan, 2012, pp. 3750-3753.

[11] R. V. Rajesh, J. Veerappan, S. K. Sujitha, and E. A. Kumar, "Classification and retrieval of images using texture features," in Computing Communication & Networking Technologies (ICCCNT), 2012 Third International Conference on, Coimbatore,India, 2012, pp. 1-5.

[12] P. Soda and G. Iannello, "Aggregation of classifiers for staining pattern recognition in antinuclear autoantibodies analysis," Information Technology in Biomedicine, IEEE Transactions on, vol. 13, pp. 322-329, 2009.

[13] A. Rigon, F. Buzzulini, P. Soda, L. Onofri, L. Arcarese, G. Iannello, et al., "Novel opportunities in automated classification of antinuclear antibodies on HEp-2 cells," Autoimmunity Reviews, vol. 10, pp. 647-652, 2011.

[14] P. Soda, G. Iannello, and M. Vento, "A multiple expert system for classifying fluorescent intensity in antinuclear autoantibodies analysis," Pattern Analysis and Applications, vol. 12, pp. 215-226, 2009.

[15] P. Elbischger, S. Geerts, K. Sander, G. Ziervogel-Lukas, and P. Sinah, "Algorithmic framework for HEp-2 fluorescence pattern classification to aid auto-immune diseases diagnosis," in Biomedical Imaging: From Nano to Macro, 2009. ISBI '09. IEEE International Symposium on, 2009, pp. 562-565.

[16] Y. Wei, C. Chang, T. Jia, and X. Xu, "Segmentation of regions of interest in lung CT images based on 2-D OTSU optimized by genetic algorithm," in Control and Decision Conference, 2009. CCDC '09. Chinese, 2009, pp. 5185-5189.

[17] H. Yu-Len, J. Yu-Lang, H. Tsu-Yi, and C. Chia-Wei, "Adaptive Automatic

Segmentation of HEp-2 Cells in Indirect Immunofluorescence Images," in Sensor Networks, Ubiquitous and Trustworthy Computing, 2008. SUTC '08. IEEE International Conference on, 2008, pp. 418-422.

[18] S. L. S. Abdullah, H. A. Hambali, and N. Jamil, "Segmentation of Natural Images Using an Improved Thresholding-Based Technique," Procedia Engineering, vol. 41, pp. 938-944, // 2012.

[19] W. S. Gan, "Application of neural networks to the processing of medical images," in Neural Networks, 1991. 1991 IEEE International Joint Conference on, 1991, pp. 300-306 vol.1.

[20] J. M. Gauch, "Image segmentation and analysis via multiscale gradient watershed hierarchies," Image Processing, IEEE Transactions on, vol. 8, pp. 69-79, 1999.

[21] A. N. Rao, V. V. Kumar, and C. Nagaraju, "A New Segmentation Method using Watersheds on Grey Level Images," in Advanced Computing and Communications, 2006. ADCOM 2006. International Conference on, 2006, pp. 275-278.

[22] A. N. Moga and M. Gabbouj, "Parallel image component labelling with watershed transformation," Pattern Analysis and Machine Intelligence, IEEE Transactions on, vol. 19, pp. 441-450, 1997.

[23] R. Nock and F. Nielsen, "Statistical region merging," Pattern Analysis and Machine Intelligence, IEEE Transactions on, vol. 26, pp. 1452-1458, 2004.

[24] C. R. Jung and J. Scharcanski, "Robust watershed segmentation using wavelets," Image and Vision Computing, vol. 23, pp. 661-669, 7/1/ 2005.

[25] P. Bo, D. Zhang, and D. Zhang, "Automatic Image Segmentation by Dynamic Region Merging," Image Processing, IEEE Transactions on, vol. 20, pp. 3592-3605, 2011.

[26] S. Ghosh and V. Chaudhary, "Feature analysis for automatic classification of HEp-2 florescence patterns : Computer-Aided Diagnosis of Auto-immune diseases," 2012, pp. 174-177.

[27] R. Guest and O. Miguel-Hurtado, "Enhancing static biometric signature verification using Speeded-Up Robust Features," in Security Technology (ICCST), 2012 IEEE International Carnahan Conference on, 2012, pp. 213-217.

[28] P. Elbischger, S. Geerts, K. Sander, G. Ziervogel-Lukas, and P. Sinah, "Algorithmic framework for HEp-2 fluorescence pattern classification to aid auto-immune diseases diagnosis," in Biomedical Imaging: From Nano to Macro, 2009. ISBI '09. IEEE International Symposium on, 2009, pp. 562-565.

[29] R. M. Haralick, K. Shanmugam, and I. H. Dinstein, "Textural Features for Image Classification," Systems, Man and Cybernetics, IEEE Transactions on, vol. SMC-3, pp. 610-621, 1973.

[30] Z. Guangyuan, G. Fei, L. Cong, L. Wei, and Y. Huai, "A pedestrian detection method based on SVM classifier and optimized Histograms of Oriented Gradients feature," in Natural Computation (ICNC), 2010 Sixth International Conference on, 2010, pp. 3257-3260.

[31] S. Singh, R. Maurya, and A. Mittal, "Application of Complete Local Binary Pattern Method for facial expression recognition," in Intelligent Human Computer Interaction (IHCI), 2012 4th International Conference on, 2012, pp. 1-4.

[32] A. Tahmasebi, H. Pourghassem, and H. Mahdavi-Nasab, "An Ear Identification System Using Local-Gabor Features and KNN Classifier," in Machine Vision and Image Processing (MVIP), 2011 7th Iranian, 2011, pp. 1-4.

[33] O. Lahdenoja, M. Laiho, and A. Paasio, "Local binary pattern feature vector extraction with CNN," in Cellular Neural Networks and Their Applications, 2005 9th International Workshop on, 2005, pp. 202-205.

[34] G. Srinivasan and G. Shobha, "Statistical texture analysis," proceedings of world academy of science, engg & tech, vol. 36, 2008.

[35] A. Materka and M. Strzelecki, "Texture analysis methods-a review," Technical

university of lodz, institute of electronics, COST B11 report, Brussels, pp. 9-11, 1998.

[36] R. Maini and H. Aggarwal, "Study and comparison of various image edge detection techniques," International Journal of Image Processing (IJIP), vol. 3, pp. 1-11, 2009.

[37] J. R. Jang, MATLAB: Fuzzy Logic Toolbox User's Guide: Version 1: Math Works, 1997.

[38] E. Sivasankar and R. Rajesh, "Knowledge discovery in medical datasets using a fuzzy logic rule based classifier," in Electronic Computer Technology (ICECT), 2010 International Conference on, Kuala Lumpur,Malaysia, 2010, pp. 208-213.

[39] J. Cervantes, L. XiaoOu, and Y. Wen, "SVM Classification for Large Data Sets by Considering Models of Classes Distribution," in Artificial Intelligence - Special Session, 2007. MICAI 2007. Sixth Mexican International Conference on, 2007, pp. 51-60.

[40] A. Mathur and G. M. Foody, "Multiclass and Binary SVM Classification: Implications for Training and Classification Users," Geoscience and Remote Sensing Letters, IEEE, vol. 5, pp. 241-245, 2008.

[41] Z. Guoqing and X. Shengyun, "Comparison of object-oriented and Maximum Likelihood Classification of land use in Karst area," in Geoscience and Remote Sensing Symposium (IGARSS), 2012 IEEE International, 2012, pp. 6099-6102.

[42] T. Hill and P. Lewicki, Statistics: Methods and Applications : a Comprehensive Reference for Science, Industry, and Data Mining: StatSoft, 2006.

[43] M. Ogrendik, "Rheumatoid arthritis is an autoimmune disease caused by periodontal pathogens," *International Journal of General Medicine,* vol. 2013, pp. 383-386, May 2013 2013.

[44] S. Anam, E. Uchino, H. Misawa, and N. Suetake, "Automatic bone boundary detection in hand radiographs by using modified level set method and diffusion filter," in *Computational Intelligence & Applications (IWCIA), 2013 IEEE Sixth International Workshop on*, 2013, pp. 51-55.

[45] P. Parascandolo, L. Cesario, L. Vosilla, M. Pitikakis, and G. Viano, "Smart Brush: A real time segmentation tool for 3D medical images," in *Image and Signal Processing and Analysis (ISPA), 2013 8th International Symposium on*, 2013, pp. 689-694.

[46] K. K. Leung, R. A. Heckemann, N. Saeed, K. J. Brooks, J. B. Buckton, K. Changani*, et al.*, "Analysis of serial MR images of joints," in *Biomedical Imaging: Nano to Macro, 2004. IEEE International Symposium on*, 2004, pp. 221-224 Vol. 1.

[47] U. Mahmood, "Near infrared optical applications in molecular imaging," *Engineering in Medicine and Biology Magazine, IEEE,* vol. 23, pp. 58-66, 2004.

[48] Y. Sasaki, R. Emori, H. Inage, T. Yuasa, M. Takagi, A. Ishikawa*, et al.*, "Preliminary image experiment using near-infrared optical computed tomography for early diagnosis of rheumatoid arthritis," in *Biomedical Engineering, 2003. IEEE EMBS Asian-Pacific Conference on*, 2003, pp. 312-313.

APPENDICES

A1. STUDY PLAN - KEY MILESTONE

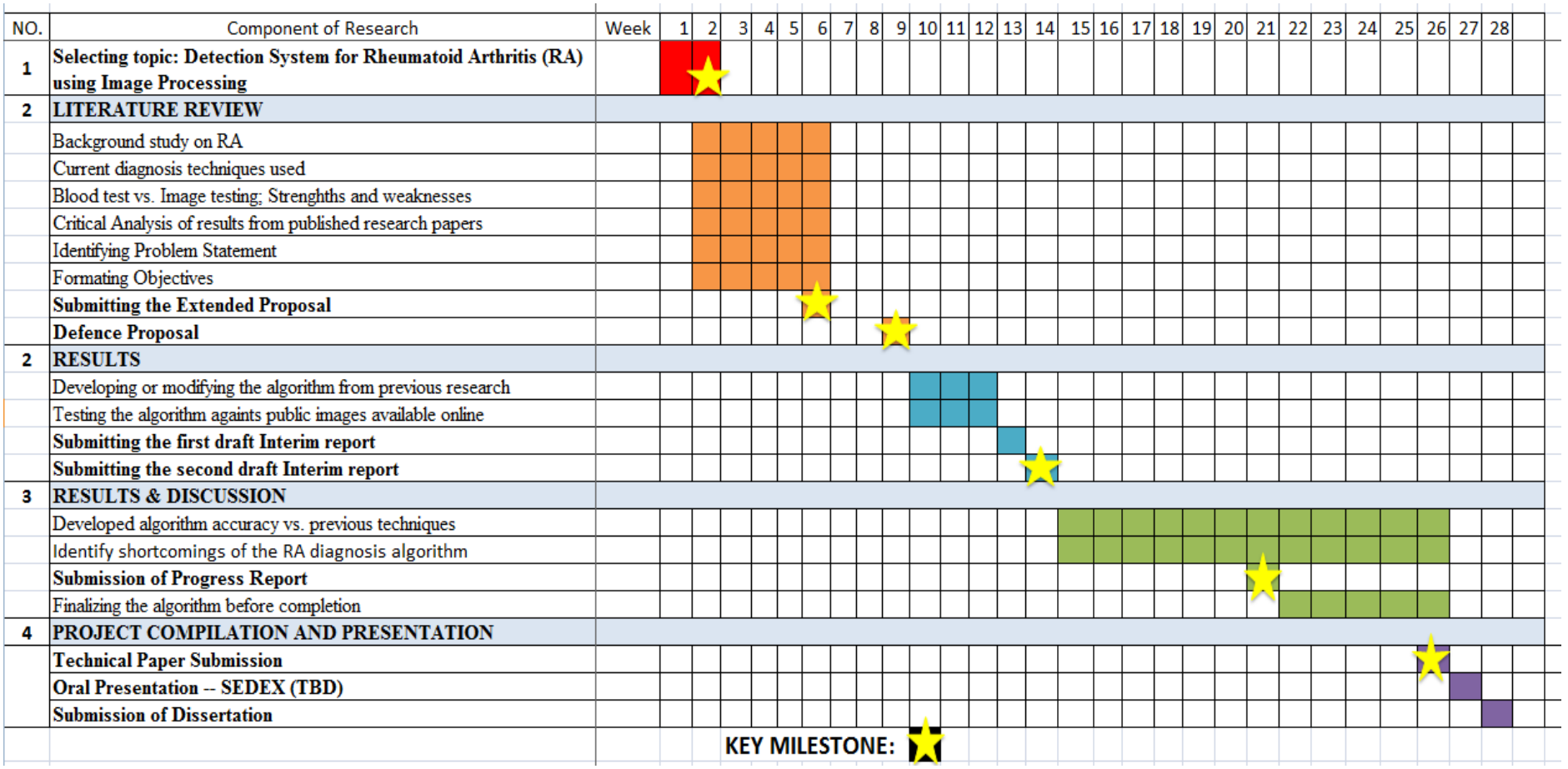

A2. Coding For Feature Extraction And Pattern Classification

```
clear all;
clc;
features = [];
%% PREPROCESSING
NF = 621;  %choose the number of images as input
prefix_image='';  %change the desired input image name
fileformat='.png';  %change the desired input image

for num= 101:721
I = imread(strcat('D:\1\info\FYP II\MIVIA_HEp-
2_Images_Dataset\MIVIA_HEp-
2_Images_Dataset\ICPR2012_Cells_Classification_Contest\training\',
int2str(num),'.png'));
%imread(strcat(prefix_image,num2str(num),fileformat));
ImageGrey = rgb2gray(I);

%% %% First-order statistics
A=double(ImageGrey);
Mean = mean(ImageGrey(:));
Variance = var(A(:));
StdDev = sqrt(Variance(:));
Entropy = entropy(ImageGrey);
%% GLCM
offsets1 = [0 1;-1 1;-1 0;-1 -1];
glcm = graycomatrix (ImageGrey, 'GrayLimits', [0 255], 'NumLevels',
8, 'Offset',offsets1, 'Symmetric', true);
stats = graycoprops (glcm, 'contrast');
stats2 = graycoprops (glcm, 'correlation');
stats3 = graycoprops (glcm, 'energy');
stats4 = graycoprops (glcm, 'homogeneity');
t = struct2array(stats);
t2 = struct2array(stats2);
t3 = struct2array(stats3);
t4 = struct2array(stats4);
Contrast = mean(t);
Correlation = mean(t2);
Energy = mean(t3);
Homogeneity = mean(t4);
%% Saving Data
features = [features; Mean StdDev Entropy Contrast Correlation
Energy Homogeneity];
%% Fuzzy Logic
fismat = readfis('Classification');
out = evalfis([Mean StdDev Entropy Contrast Correlation Energy
Homogeneity],fismat);
fprintf('%d\t Output = %0.3f \n',num,out);
if out<0.201
disp('The staining pattern is homogeneous')
elseif out<0.401
disp('The staining pattern is fine speckled')
elseif out<0.601
disp('The staining pattern is coarse speckled')
elseif out<0.801
disp('The staining pattern is centromere')
else
disp('The staining pattern is nucleolar')
end
end
```

	Pattern	Mean	Std. Dev.	Entropy	Contrast	Correlation	Energy	Homogeneity
1	fine_speckled	43.72811791	11.93924111	5.114335723	0.025839567	0.915829561	0.667212833	0.987080217
2	nucleolar	20.77861685	16.99048077	4.627876221	0.048252781	0.913903169	0.700768785	0.97591882
3	cytoplasmatic	39.75857143	18.21375548	5.681766575	0.110493549	0.894554935	0.325697561	0.944753225
4	centromere	21.18746471	12.49985485	5.047751692	0.077884374	0.775614573	0.688015273	0.962163428
5	fine_speckled	15.33712121	3.28594115	3.409838056	0	NaN	1	1
6	centromere	13.17992231	3.002032998	3.490618867	0	NaN	1	1
7	coarse_speckled	19.3931781	4.27569161	4.054285008	0.005225272	0.580704211	0.982358876	0.997387364
8	nucleolar	11.22551487	3.257505355	3.503909861	0	NaN	1	1
9	nucleolar	19.0628695	11.24228152	4.59495884	0.02220015	0.904634837	0.75876013	0.988899925
10	fine_speckled	33.55211158	12.19268959	5.38273794	0.031294975	0.933833148	0.496491227	0.984352512
11	centromere	10.86192389	2.515761678	2.938901009	0	NaN	1	1
12	homogeneous	13.00204248	2.766971435	3.10964166	0	NaN	1	1
13	homogeneous	54.48732057	20.93977789	5.837371014	0.050689441	0.960268767	0.33863632	0.974655279
14	centromere	17.5843777	12.64784678	4.775213011	0.057155518	0.803216279	0.780530243	0.972486312
15	homogeneous	33.85561293	6.430964505	4.578955941	0.083389993	0.783222746	0.538501628	0.958305004
16	fine_speckled	39.4707161	14.36825519	5.485672173	0.034371863	0.926132766	0.516823049	0.982814069
17	homogeneous	14.29006656	4.517065454	3.847216877	0	NaN	1	1
18	homogeneous	34.41931362	8.77214287	4.667540638	0.0350759	0.911514676	0.568893831	0.98246205
19	fine_speckled	15.02238916	3.498644338	3.556036393	0	NaN	1	1
20	centromere	27.41820221	17.36804875	5.497864693	0.11630423	0.842101816	0.514814178	0.943378496
21	coarse_speckled	47.59703146	17.47283036	5.954567264	0.114345413	0.86918822	0.336544372	0.942827294
22	centromere	9.615131579	2.533714366	3.240525686	0	NaN	1	1
23	centromere	19.15399096	10.97219261	4.724914097	0.067082372	0.745617692	0.727671722	0.966458814
24	fine_speckled	36.26309524	12.48191577	5.216668999	0.027647617	0.938550736	0.522908237	0.986176192
25	homogeneous	33.99799908	8.572738018	4.683040589	0.034378629	0.917239703	0.550901296	0.982810685
26	centromere	10.75878443	2.3529875	2.817928407	0	NaN	1	1

27	coarse_speckled	46.84882629	18.96163088	6.014453789	0.11827308	0.879315918	0.305512858	0.94086346
28	nucleolar	12.01434599	4.204507496	3.794988665	0.001376995	0.124827839	0.999226195	0.999770501
29	centromere	13.21428571	4.46077501	3.685213301	0.002734151	0.783591776	0.990712761	0.998632925
30	fine_speckled	37.06006006	11.4943736	5.314988687	0.033797979	0.920843807	0.539864988	0.98310101
31	centromere	10.82594086	3.114002263	3.442763367	0	NaN	1	1
32	cytoplasmatic	41.32618465	25.27978155	6.056487453	0.108654329	0.931971296	0.319992852	0.94580802
33	centromere	10.61638554	2.725142643	2.980524142	0.000819812	0.374589825	0.997871721	0.999590094
34	centromere	17.28974185	10.94596911	4.593326501	0.0571246	0.744324111	0.783878968	0.971669048
35	centromere	11.41295689	2.696334533	3.092007597	0.000238166	-0.000119097	0.999523753	0.999880917
36	centromere	19.13239326	11.88139643	4.96109775	0.079922169	0.722582083	0.694937857	0.960507086
37	fine_speckled	36.75324675	12.40663811	5.394583248	0.036024736	0.917789207	0.526604604	0.981987632
38	centromere	20.47442455	12.47534282	4.910257742	0.083351156	0.749988817	0.669648775	0.958616016
39	cytoplasmatic	30.21862132	17.16354935	5.237875915	0.060883317	0.921391414	0.497228194	0.969558342
40	nucleolar	12.54599567	3.227376667	3.440093571	0	NaN	1	1
41	homogeneous	61.98470564	23.08159796	6.03818627	0.044515355	0.961865502	0.409253677	0.977742322
42	nucleolar	10.16825397	2.109954765	3.016567541	0	NaN	1	1
43	coarse_speckled	19.20888889	5.049258541	4.309568285	0.012741988	0.574699424	0.957495165	0.993629006
44	centromere	14.10843373	4.865834636	3.99567037	0.000798293	0.374600598	0.997927522	0.999600853
45	coarse_speckled	46.3718947	15.71782032	5.814055368	0.122855659	0.812045057	0.411898085	0.93857217
46	centromere	12.38167013	3.703117512	3.655030296	0	NaN	1	1
47	nucleolar	20.02169275	12.57493529	4.627538951	0.036956975	0.883780828	0.712827106	0.981521513
48	coarse_speckled	20.3588256	4.322025917	4.08809794	0.008348708	0.587887746	0.971483345	0.995825646
49	homogeneous	38.38447594	9.335901676	4.831204702	0.029055269	0.919834099	0.608646908	0.985472365
50	homogeneous	12.11173309	2.456576756	3.095017931	0	NaN	1	1
51	cytoplasmatic	37.43772317	18.13868788	5.46681853	0.104883476	0.901549204	0.36927188	0.947724144

52	centromere	20.99429563	10.68401	4.877815009	0.075794565	0.733442441	0.680439116	0.962102717
53	centromere	16.20363636	7.664604211	4.295018776	0.043810653	0.624241167	0.846010714	0.978094673
54	coarse_speckled	17.53005818	3.219067382	3.680060834	0	NaN	1	1
55	coarse_speckled	42.01171275	14.62599666	5.719308941	0.070433447	0.877283642	0.465860751	0.964783277
56	homogeneous	89.37504628	39.32664626	6.891092126	0.130913721	0.959146307	0.192578736	0.93454314
57	centromere	10.04523402	2.622390466	2.959514092	0	NaN	1	1
58	coarse_speckled	18.32570732	3.31001214	3.746782115	0	NaN	1	1
59	fine_speckled	37.26929359	13.30346547	5.484565491	0.038695268	0.910466935	0.530596196	0.980652366
60	homogeneous	35.86342593	8.677824915	4.736585699	0.037340172	0.901834209	0.583082882	0.981329914
61	centromere	18.85854256	8.906677474	4.742889332	0.063175247	0.663209517	0.7564944	0.968412376
62	coarse_speckled	49.67194781	16.94084807	5.943801021	0.121219248	0.857442393	0.336437337	0.939390376
63	nucleolar	19.86586057	11.04013123	4.891552254	0.036694093	0.855464083	0.80032858	0.981652954
64	centromere	14.05025196	7.210121679	4.070087418	0.024361542	0.697074033	0.901922186	0.987819229
65	nucleolar	13.53316419	4.174493594	3.891704226	0	NaN	1	1
66	fine_speckled	16.64975845	4.118649481	3.889568107	0	NaN	1	1
67	homogeneous	10.02280551	2.061648458	2.975094357	0	NaN	1	1
68	nucleolar	12.24904025	2.983070473	3.415304408	0	NaN	1	1
69	coarse_speckled	40.64138105	12.45489655	5.45296289	0.051949653	0.881173443	0.548697086	0.974025174
70	coarse_speckled	18.24938353	3.786923562	3.892249108	0	NaN	1	1
71	centromere	17.65277274	9.812199874	4.730448253	0.054835357	0.704692959	0.774759099	0.972582321
72	coarse_speckled	39.68272569	14.24414354	5.591421968	0.064708467	0.874675343	0.488214685	0.967645767
73	nucleolar	19.87630522	11.09330495	4.652625455	0.025908485	0.897082759	0.725753833	0.987045758
74	fine_speckled	36.7736411	11.40789184	5.260622399	0.034771271	0.917902601	0.54236575	0.982614364
75	nucleolar	11.33714431	2.604571175	3.190837887	0	NaN	1	1
76	homogeneous	49.22795851	23.62145254	6.082341581	0.048777642	0.965269413	0.306455023	0.975611179

77	homogeneous	16.89580673	6.365930095	4.446156614	0	NaN	1	1
78	coarse_speckled	16.5144391	3.467183519	3.771609235	0.000377929	-0.000189	0.999244357	0.999811036
79	centromere	10.246875	2.219313216	3.064397921	0	NaN	1	1
80	homogeneous	33.53916645	6.194815169	4.553895789	0.067141965	0.842668072	0.510538203	0.966429017
81	centromere	10.91722944	2.830460387	3.068637704	0	NaN	1	1
82	homogeneous	14.48883162	4.880193289	3.853322288	0.002920071	0.374634778	0.99810461	0.999513321
83	nucleolar	16.05952381	12.44249708	4.284600702	0.025981962	0.896197748	0.802912467	0.987009019
84	centromere	12.58147321	2.37508944	3.141747241	0	NaN	1	1
85	nucleolar	19.73782772	10.2978008	4.690860085	0.026843118	0.887576693	0.769116486	0.986578441
86	coarse_speckled	17.71099784	3.071531897	3.620944569	0	NaN	1	1
87	homogeneous	33.71751335	9.077892865	4.525210981	0.031900278	0.919612947	0.578531293	0.984980632
88	homogeneous	12.71889401	3.084946159	3.305343339	0	NaN	1	1
89	coarse_speckled	35.99875467	12.1834295	5.39452288	0.061966921	0.863071065	0.502054556	0.96901654
90	nucleolar	21.61813809	9.149902936	4.895818187	0.03842584	0.845334888	0.731745187	0.98078708
91	coarse_speckled	42.38634886	16.72370478	5.74277045	0.097607399	0.875493211	0.36833113	0.9511963
92	centromere	19.55952381	13.34422234	4.832807088	0.078810166	0.786062083	0.715326456	0.962256737
93	fine_speckled	33.32620993	12.21327312	5.299344326	0.03686771	0.91970733	0.505564347	0.981619865
94	nucleolar	12.7504529	3.451329393	3.547997767	0	NaN	1	1
95	fine_speckled	25.21210076	5.911590662	4.368347454	0.04603577	0.812690859	0.710587537	0.976982115
96	homogeneous	11.50900901	2.833657298	3.327585361	0	NaN	1	1
97	centromere	15.05532787	6.288341572	4.260462681	0.01947121	0.648206349	0.9256132	0.990264395
98	homogeneous	59.10235832	26.16659242	6.078085703	0.081495588	0.953121502	0.269284281	0.959252206
99	centromere	11.19365079	2.929040965	3.453050089	0	NaN	1	1
100	centromere	27.54884005	12.77475069	5.432693494	0.104102614	0.789643903	0.477029563	0.947948693
101	nucleolar	18.08776371	11.97964018	4.531481662	0.025871952	0.890798686	0.741910461	0.987064024

102	centromere	18.97927181	11.87992488	4.842791723	0.072373728	0.750256108	0.705758424	0.964489678
103	cytoplasmatic	27.82329517	15.27702206	5.187965308	0.060882809	0.90220596	0.582529664	0.969568473
104	coarse_speckled	19.99431818	4.049413389	3.986400183	0.002756574	0.284333334	0.993403311	0.998621713
105	homogeneous	16.87378336	6.257198986	4.302002801	0	NaN	1	1
106	centromere	10.95975976	2.636489348	2.808174997	0.000765796	0.374616867	0.998011807	0.999617102
107	centromere	9.50335871	2.775427369	3.150806534	0	NaN	1	1
108	fine_speckled	34.57676768	12.80023812	5.509977318	0.037919675	0.917009419	0.506756875	0.981040163
109	homogeneous	12.7802897	2.928390083	3.182258861	0	NaN	1	1
110	nucleolar	11.33687226	2.859647132	3.431220476	0	NaN	1	1
111	coarse_speckled	46.72175981	17.97262179	5.946786746	0.122171281	0.864313974	0.327330644	0.938914359
112	homogeneous	63.2560208	28.65922245	6.256993642	0.080360522	0.957613601	0.251991452	0.959819739
113	nucleolar	19.51071761	11.47542484	4.765576216	0.031214654	0.8701564	0.733378642	0.984392673
114	fine_speckled	40.41269992	15.07323184	5.519321104	0.023903984	0.942017229	0.584365222	0.988048008
115	homogeneous	60.4714409	27.12249926	6.360745064	0.085928227	0.949052966	0.265295993	0.957035886
116	cytoplasmatic	33.68466403	17.35419146	5.549096039	0.090926065	0.892130657	0.414641625	0.954603725
117	coarse_speckled	26.3775454	7.923915856	4.859264381	0.085647658	0.796383992	0.501395206	0.957176171
118	homogeneous	32.11269956	8.615417219	4.626088814	0.033081622	0.924152393	0.531697139	0.983459189
119	centromere	15.41684211	6.890295974	4.295667414	0.029734217	0.640017754	0.888696827	0.985132891
120	centromere	21.41618337	10.12853596	4.988722356	0.068581824	0.746229182	0.67744792	0.965709088
121	centromere	22.04481793	11.23457144	5.028087274	0.080970548	0.753606753	0.638313865	0.959514726
122	homogeneous	86.76977433	38.69224141	7.036309316	0.10324202	0.967588231	0.173232056	0.94837899
123	centromere	11.17859944	2.407018362	2.961076857	0	NaN	1	1
124	homogeneous	36.45716423	9.459269098	4.750885181	0.033314961	0.909115899	0.600406161	0.98334252
125	centromere	10.12182663	2.205607375	2.827129752	0	NaN	1	1
126	coarse_speckled	40.75990538	15.3955875	5.637060077	0.062331102	0.891129121	0.464492221	0.968834449

127	homogeneous	55.63653403	28.68970987	6.279061536	0.08418884	0.956291026	0.25905658	0.95790558
128	coarse_speckled	45.89497942	18.9747896	5.926964098	0.104907032	0.896217396	0.305655484	0.947546484
129	coarse_speckled	41.19017857	12.9564565	5.543703854	0.072675308	0.848399117	0.503948508	0.963662346
130	homogeneous	41.37273143	6.872443719	4.680996316	0.016674525	0.907490611	0.803120151	0.991662738
131	centromere	22.41769547	11.85129511	5.048289721	0.071442733	0.792980451	0.642363019	0.964278634
132	nucleolar	17.95213868	11.40943661	4.471709601	0.023413296	0.904852919	0.743904746	0.988293352
133	nucleolar	14.98664344	4.817321034	3.907163217	0.002600143	0.540362897	0.991755987	0.998699929
134	centromere	21.84683099	10.81602133	5.07404473	0.078013838	0.745490876	0.660066723	0.96106015
135	homogeneous	66.56394582	25.39768478	6.216609422	0.064743824	0.952898489	0.345295789	0.967628088
136	homogeneous	52.13772049	23.59471207	6.026974371	0.050704152	0.963906709	0.316806005	0.974647924
137	cytoplasmatic	22.9566524	11.50369829	4.577570782	0.036293937	0.89296004	0.695474774	0.981914328
138	nucleolar	22.19051633	12.00128026	4.921178103	0.031596147	0.901738358	0.66692725	0.984201926
139	nucleolar	10.50232794	2.618232584	3.206885467	0	NaN	1	1
140	nucleolar	18.03772636	8.821677137	4.537630665	0.022338925	0.874521433	0.800317326	0.988830538
141	coarse_speckled	29.58576682	8.658027086	4.985421936	0.078152888	0.843172737	0.429800613	0.960923556
142	nucleolar	12.70789474	3.293916588	3.57170358	0	NaN	1	1
143	nucleolar	13.31435705	4.048008331	3.742583972	0.000571713	0.249714035	0.998667109	0.999714144
144	coarse_speckled	18.57729469	3.409279627	3.775926442	0.00035202	-0.000176041	0.999296146	0.99982399
145	centromere	19.56668535	12.74123951	4.96300515	0.071037455	0.790362946	0.717172014	0.965006204
146	homogeneous	33.91410256	5.4652595	4.285349298	0.053869102	0.855117203	0.576599734	0.973065449
147	homogeneous	33.24402006	10.60624531	5.12022416	0.034320096	0.931319739	0.46715929	0.982839952
148	fine_speckled	41.07068869	12.76029176	5.444221203	0.032096333	0.909380085	0.614731692	0.983951834
149	centromere	16.18353504	6.099694078	4.38178647	0.000948378	0.499525361	0.997159212	0.999525811
150	centromere	11.55586473	2.777845316	3.105018686	0	NaN	1	1
151	centromere	14.31386973	5.252706447	4.111389167	0.000937999	0.399530634	0.997502565	0.999531001

152	centromere	13.01187129	3.603689758	3.606427855	0	NaN	1	1
153	centromere	10.16883117	2.958281845	3.34830392	0	NaN	1	1
154	cytoplasmatic	25.47986858	6.101566895	4.344258856	0.079715864	0.763290896	0.59008093	0.960142068
155	centromere	11.044329	3.045521568	3.160250089	0.000571332	0.458047516	0.998375923	0.999714334
156	homogeneous	40.00163332	10.35861194	4.753919206	0.026864839	0.923784163	0.620687275	0.98656758
157	fine_speckled	31.82911392	11.11537045	5.313701484	0.036061481	0.926925812	0.471655315	0.981969259
158	centromere	9.639285714	2.8917755	3.359842818	0	NaN	1	1
159	homogeneous	11.66326531	2.503539715	3.128306939	0	NaN	1	1
160	centromere	23.20757576	11.7974529	5.06643629	0.079402422	0.779020904	0.616540924	0.960298789
161	coarse_speckled	48.4548495	18.87504162	6.002281829	0.126205253	0.876177637	0.300285713	0.936897373
162	fine_speckled	17.1429953	3.01263976	3.47017362	0	NaN	1	1
163	nucleolar	19.90466352	10.38386779	4.968093769	0.035209129	0.84067468	0.785833928	0.982395436
164	cytoplasmatic	21.42188366	6.14725991	4.032944948	0.026672834	0.758947955	0.879774136	0.986663583
165	coarse_speckled	47.62637363	18.51066506	6.03135603	0.11769334	0.875527025	0.319953008	0.94115333
166	nucleolar	24.24343147	13.40303035	5.216256992	0.040652846	0.899419536	0.657778058	0.979996916
167	nucleolar	10.57844094	3.021001039	3.444167372	0	NaN	1	1
168	nucleolar	11.02447493	2.660196091	3.235699207	0	NaN	1	1
169	centromere	12.70729389	2.796631345	3.393484447	0	NaN	1	1
170	homogeneous	52.25263158	18.95953198	5.756220704	0.053035488	0.955810954	0.317190053	0.973482256
171	centromere	8.789919355	2.123296488	2.941441665	0	NaN	1	1
172	fine_speckled	36.83273566	9.609460499	5.0673546	0.0376997	0.904418771	0.568596266	0.98115015
173	fine_speckled	31.57494685	10.55476337	5.197278391	0.036015636	0.927061133	0.471411734	0.981992182
174	centromere	24.41177368	16.34072371	5.166264093	0.09972005	0.833785487	0.610825472	0.951076082
175	homogeneous	57.86391753	24.00454444	6.221047449	0.059670324	0.954764763	0.33263689	0.970164838
176	cytoplasmatic	21.80488047	3.807122784	3.765628891	0.003712367	0.817773831	0.97592221	0.998143816

177	homogeneous	38.05533199	9.87392638	4.919547366	0.033132251	0.911100496	0.594501979	0.983433874
178	fine_speckled	13.65401786	3.878658709	3.771163176	0	NaN	1	1
179	homogeneous	41.91148695	14.06320821	5.65440849	0.053957087	0.884068352	0.551051668	0.973021457
180	homogeneous	15.87088989	5.307009595	4.006687651	0	NaN	1	1
181	cytoplasmatic	35.52562486	17.33305262	5.706937207	0.091193079	0.898000852	0.37874707	0.95440346
182	homogeneous	13.95601926	2.527674701	2.947469671	0	NaN	1	1
183	homogeneous	10.80297619	1.807955217	2.850380163	0	NaN	1	1
184	fine_speckled	37.46070413	10.47978768	5.23134366	0.037408416	0.901854441	0.582277123	0.981295792
185	fine_speckled	18.17008403	4.567490842	4.024014155	0	NaN	1	1
186	coarse_speckled	44.68357257	14.09304598	5.643891563	0.076714935	0.86304942	0.488619261	0.961642532
187	fine_speckled	16.85247432	4.391126295	4.007987433	0	NaN	1	1
188	homogeneous	41.63687725	8.002705432	4.747748976	0.033256939	0.845212558	0.752052646	0.983371531
189	fine_speckled	15.74819244	3.81123533	3.813948519	0	NaN	1	1
190	coarse_speckled	17.21738489	3.528874925	3.795831671	0	NaN	1	1
191	centromere	12.03156932	4.095721386	3.806888584	0	NaN	1	1
192	homogeneous	16.87229437	4.538519255	3.90350595	0	NaN	1	1
193	coarse_speckled	38.39971014	14.42030344	5.714212727	0.066447489	0.887525627	0.440647236	0.966776255
194	homogeneous	41.08257056	11.28980547	5.11255589	0.037228878	0.896082535	0.605200685	0.981385561
195	nucleolar	17.09741917	12.08321073	4.583951887	0.021893592	0.902018393	0.759223356	0.989053204
196	centromere	19.7600387	8.509284697	4.691742162	0.062270096	0.643734658	0.76721195	0.968864952
197	coarse_speckled	18.60294118	3.676882081	3.872355491	0.002442043	0.276554688	0.994192226	0.998778978
198	centromere	16.3035982	7.598920723	4.461703557	0.037666828	0.654787588	0.854799221	0.981166586
199	coarse_speckled	29.06749482	9.067017647	5.014871546	0.085042985	0.828571213	0.426350053	0.957478507
200	homogeneous	13.29642857	3.152933613	3.451456564	0	NaN	1	1
201	centromere	11.60036199	3.816045227	3.630791963	0	NaN	1	1

202	coarse_speckled	43.13364662	14.00696774	5.666703935	0.073772075	0.849252891	0.517483811	0.963113962
203	homogeneous	12.89646384	3.450201073	3.403543181	0	NaN	1	1
204	fine_speckled	30.76786844	10.11510824	5.073180775	0.037408405	0.923877729	0.472505505	0.981295797
205	homogeneous	11.08758741	2.72557646	3.321353845	0	NaN	1	1
206	fine_speckled	21.76120581	5.562271492	4.332186411	0.01038667	0.448146678	0.970924119	0.994806665
207	centromere	9.316003617	2.64571828	3.167584503	0	NaN	1	1
208	fine_speckled	18.11317254	4.782696062	4.169703839	0	NaN	1	1
209	centromere	17.74970484	10.06749409	4.670135175	0.065739475	0.676191353	0.762777651	0.967292706
210	nucleolar	12.63078704	2.838947725	3.444509948	0	NaN	1	1
211	cytoplasmatic	36.76236542	14.83312642	5.485347833	0.101579677	0.867877115	0.367564945	0.949241727
212	cytoplasmatic	37.15426749	22.96307234	5.733378661	0.089930932	0.931598405	0.390346032	0.955034534
213	homogeneous	55.0436214	21.11017333	5.782709237	0.045118154	0.964939621	0.346970731	0.977440923
214	coarse_speckled	17.36926112	3.670136209	3.847605417	0	NaN	1	1
215	centromere	10.72426564	2.405758237	2.762412626	0	NaN	1	1
216	centromere	11.81761905	3.499970387	3.508112335	0	NaN	1	1
217	homogeneous	64.48711129	30.67754642	6.497299417	0.073367853	0.966057015	0.241278828	0.963316074
218	coarse_speckled	46.63118581	14.64927154	5.75398291	0.098419448	0.834698548	0.459138491	0.950790276
219	centromere	19.10688121	9.73547609	4.555450237	0.052765274	0.748159819	0.791268572	0.973706609
220	centromere	12.4268556	3.182250506	3.533057351	0	NaN	1	1
221	centromere	12.3405339	4.08861754	3.652005562	0.00358837	0.374551132	0.997671339	0.999401938
222	homogeneous	42.60202438	8.218869535	4.802505887	0.017490142	0.898626515	0.809857962	0.991254929
223	cytoplasmatic	22.65015559	5.505037954	4.103864402	0.044607514	0.606613666	0.844044826	0.977696243
224	centromere	20.19166667	11.13595599	4.844402583	0.091043142	0.686617572	0.692834067	0.954549945
225	cytoplasmatic	21.77891112	2.70038794	3.383271204	0.001842984	0.54746372	0.994090789	0.999078508
226	fine_speckled	31.90826538	10.14794721	5.225584799	0.047908115	0.90100434	0.47028126	0.976045942

227	nucleolar	18.41380266	11.97900904	4.733362905	0.027041531	0.882750496	0.758369184	0.986479235
228	cytoplasmatic	29.43640128	12.05863396	5.131271399	0.069502847	0.861400235	0.520239244	0.965248576
229	nucleolar	18.1503792	11.85768117	4.610517965	0.028621609	0.882232038	0.72947429	0.985689195
230	centromere	9.839171624	3.023508424	3.373231313	0	NaN	1	1
231	homogeneous	31.89174129	7.460473168	4.593283743	0.045990084	0.9029162	0.482184029	0.977004958
232	homogeneous	37.30943089	7.241441166	4.670832165	0.022315229	0.920427988	0.697147944	0.988842386
233	homogeneous	34.77590361	6.638677683	4.670184509	0.090255875	0.776676308	0.513679537	0.954872062
234	fine_speckled	18.05408497	5.897211524	4.464966595	0.001834633	0.632413716	0.99318345	0.999082684
235	fine_speckled	13.92953523	1.887614062	2.744511492	0	NaN	1	1
236	centromere	18.15392934	8.302385776	4.600042893	0.05239963	0.659719196	0.798014352	0.973800185
237	centromere	11.22783389	2.567879849	2.84469655	0	NaN	1	1
238	cytoplasmatic	31.11026827	13.25935302	5.219444883	0.066601996	0.88556468	0.4808605	0.966699002
239	homogeneous	44.61459489	21.72601445	6.01939354	0.04535865	0.961406424	0.318988888	0.977320675
240	centromere	20.65242215	10.68863319	4.515404045	0.065787658	0.756810875	0.715365508	0.967224626
241	centromere	12.52777778	4.349569296	3.830072551	0	NaN	1	1
242	centromere	16.84804688	8.29983372	4.3580619	0.04714248	0.66831492	0.818531386	0.97642876
243	nucleolar	17.35943775	11.90301949	4.5144758	0.018749576	0.917686953	0.759468526	0.990625212
244	nucleolar	21.06114751	11.10199989	4.910063937	0.037153303	0.880332666	0.653862939	0.981423349
245	homogeneous	48.69021325	20.77184804	6.032999423	0.054605908	0.951847041	0.311090458	0.972697046
246	centromere	23.1201341	13.76584248	5.194018013	0.085316907	0.80488275	0.646724921	0.95778638
247	nucleolar	11.49058085	3.231331514	3.576813012	0	NaN	1	1
248	coarse_speckled	27.18732194	7.969175998	4.914228163	0.084221334	0.810363075	0.479198977	0.957889333
249	homogeneous	52.13180778	20.28035609	5.876723441	0.070349152	0.94336785	0.302080845	0.964825424
250	centromere	17.65636105	7.670453912	4.711309623	0.014067204	0.597430847	0.951232776	0.992966398
251	cytoplasmatic	25.42347115	14.72319354	5.001857577	0.051342607	0.901662414	0.613442304	0.974328696

252	centromere	9.903958333	3.151806978	3.490640166	0	NaN	1	1
253	centromere	22.6440678	12.67953802	5.078816337	0.089030894	0.76801254	0.636214443	0.955545693
254	homogeneous	15.45449827	4.720296202	3.974768975	0	NaN	1	1
255	coarse_speckled	17.79340883	3.51728336	3.785644343	0	NaN	1	1
256	homogeneous	20.80149502	7.771958739	4.572538025	0.005854098	0.368271382	0.984925572	0.997072951
257	nucleolar	14.38434783	3.809698215	3.601132058	0	NaN	1	1
258	fine_speckled	32.52088816	10.16890864	5.172841464	0.042299689	0.911347789	0.482170326	0.978850155
259	nucleolar	14.62753784	2.958028076	3.435168273	0	NaN	1	1
260	nucleolar	11.35668073	2.560272397	3.126118052	0	NaN	1	1
261	coarse_speckled	46.64966216	15.66197353	5.772991702	0.103333813	0.860022633	0.389128497	0.948333094
262	nucleolar	11.53194263	3.513621286	3.694168968	0	NaN	1	1
263	homogeneous	59.07776561	21.99379317	6.009353697	0.048993037	0.958656479	0.366994153	0.975503481
264	nucleolar	21.01464941	13.67064059	4.880018605	0.034136816	0.908420684	0.707373462	0.982931592
265	homogeneous	12.98367859	2.830710219	3.267636854	0	NaN	1	1
266	coarse_speckled	32.91073124	9.448738511	5.15675463	0.071699876	0.852284094	0.447919957	0.964150062
267	coarse_speckled	30.49721293	9.622859041	5.124793883	0.071630309	0.857408381	0.434899561	0.964184845
268	nucleolar	15.3989425	8.885754643	4.173991919	0.016559541	0.908027363	0.803826182	0.991720229
269	homogeneous	61.6826087	25.56994408	6.477766616	0.112846381	0.929497848	0.242530088	0.943576809
270	coarse_speckled	17.79658034	4.181306362	4.062381275	0.001087319	0.527233492	0.996614734	0.999456341
271	homogeneous	50.24733333	24.27485745	6.164919328	0.056095407	0.960319028	0.300017251	0.971952296
272	centromere	14.8182574	4.299226129	3.872499609	0	NaN	1	1
273	centromere	12.149	3.028354191	3.448112518	0	NaN	1	1
274	coarse_speckled	45.51147461	16.60567198	5.840006258	0.10981887	0.865543739	0.363774998	0.947668323
275	fine_speckled	15.14100346	3.914504888	3.790687454	0	NaN	1	1
276	centromere	12.23924513	3.85154096	3.666175846	0	NaN	1	1

277	cytoplasmatic	26.36444788	7.035654461	4.425705204	0.078832528	0.808048735	0.516901643	0.960583736
278	homogeneous	60.34771825	23.9063528	6.164663724	0.050615788	0.959632763	0.366477271	0.974692106
279	centromere	10.56472574	2.562534158	2.901593037	0	NaN	1	1
280	fine_speckled	15.87763158	4.386215031	3.966388744	0	NaN	1	1
281	coarse_speckled	17.98580122	3.131949475	3.657854791	0	NaN	1	1
282	centromere	9.540692008	2.548348207	3.256230529	0	NaN	1	1
283	nucleolar	11.04566104	2.467356802	3.170634149	0	NaN	1	1
284	centromere	8.665935031	2.169722453	2.973147626	0	NaN	1	1
285	homogeneous	44.64322251	12.55874921	5.555579295	0.075672909	0.802598557	0.600341912	0.962163546
286	homogeneous	13.55197483	3.448577428	3.365868959	0	NaN	1	1
287	fine_speckled	36.06940223	12.6303111	5.359374044	0.030332716	0.93240581	0.521469293	0.984833642
288	nucleolar	13.80504511	3.884237315	3.726414642	0	NaN	1	1
289	nucleolar	13.46146045	3.334665715	3.63411614	0	NaN	1	1
290	fine_speckled	23.66607818	5.001460118	4.208809689	0.017724687	0.862678738	0.853717688	0.991137656
291	homogeneous	35.74840619	8.490794898	4.857653633	0.040930907	0.906244286	0.523656913	0.979534546
292	centromere	10.25538948	3.265263863	3.501334617	0	NaN	1	1
293	nucleolar	19.87401781	11.15605095	4.718104947	0.030406583	0.880138094	0.723468541	0.984796708
294	coarse_speckled	17.92338102	3.90731963	3.951698064	0.002790397	0.339510932	0.992997521	0.998604801
295	centromere	19.4673578	14.57730474	4.615300796	0.074468623	0.827024628	0.744778968	0.965188436
296	fine_speckled	23.92690394	4.936769129	4.20288616	0.022897275	0.804403421	0.860754187	0.988551363
297	fine_speckled	55.25360977	10.92017589	5.277194712	0.048276239	0.897063575	0.54461675	0.975861881
298	nucleolar	19.10556787	11.84488953	4.726343513	0.024826218	0.892343	0.759436827	0.987586891
299	centromere	13.91297262	3.627512532	3.73370202	0	NaN	1	1
300	centromere	13.22666667	2.28915318	3.166906177	0	NaN	1	1
301	nucleolar	19.33855072	11.91292707	4.808826449	0.024695341	0.907991165	0.74520118	0.987652329

302	fine_speckled	24.58379784	5.8615271	4.447718569	0.030578969	0.858523764	0.754497078	0.984710515
303	fine_speckled	15.73717949	3.74479579	3.696757632	0	NaN	1	1
304	homogeneous	13.78552327	3.330868265	3.511208253	0	NaN	1	1
305	centromere	22.93929412	13.24453944	5.122473729	0.088356057	0.791643471	0.59767361	0.955821972
306	centromere	14.8448235	4.021369441	3.760794301	0.000667252	0.166332905	0.99854596	0.999666374
307	centromere	11.01741788	2.23038908	2.712550373	0	NaN	1	1
308	coarse_speckled	20.74663073	4.77156336	4.222038174	0.014110414	0.594380104	0.951340881	0.992944793
309	coarse_speckled	18.83307142	3.489929033	3.798550698	0	NaN	1	1
310	coarse_speckled	17.38006757	2.723697828	3.440326124	0	NaN	1	1
311	nucleolar	17.49487952	8.068540417	4.468761671	0.022345231	0.848485797	0.830825461	0.988827384
312	centromere	20.93079073	12.90223185	4.926503515	0.077776584	0.788353819	0.709355102	0.9622327
313	homogeneous	37.34289491	9.337384209	4.982549619	0.023791842	0.925843772	0.655396128	0.988104079
314	cytoplasmatic	21.01166089	4.5298286	3.798998924	0.019229251	0.628830441	0.929358595	0.990385374
315	nucleolar	19.095	11.79110352	4.61070209	0.032187925	0.874248748	0.721231444	0.983906038
316	nucleolar	14.49370416	2.801794123	3.323500418	0	NaN	1	1
317	coarse_speckled	28.11949807	9.714390473	5.027243893	0.068582106	0.86012477	0.44606407	0.965708947
318	centromere	10.51945181	2.557804315	2.874859624	0	NaN	1	1
319	cytoplasmatic	28.6441349	12.13235727	5.227288821	0.067816528	0.859947334	0.508530043	0.966091736
320	nucleolar	9.609356725	1.739378862	2.728273107	0	NaN	1	1
321	nucleolar	19.07404181	12.86196458	4.745126829	0.034429127	0.899621631	0.69122373	0.982785437
322	centromere	8.590812173	2.559232558	3.131905632	0	NaN	1	1
323	homogeneous	59.81321839	26.71500067	6.375669042	0.06179452	0.963208824	0.29372828	0.96910274
324	centromere	9.962411348	2.99952796	3.417066094	0	NaN	1	1
325	homogeneous	18.00813802	6.093706281	4.260369306	0.005154379	0.445954805	0.996929879	0.999134483
326	fine_speckled	22.69059011	6.314265541	4.563220034	0.026616407	0.829350923	0.818354106	0.986691797

327	nucleolar	10.39110894	2.800433237	3.203668405	0	NaN	1	1
328	centromere	11.44626758	3.42368791	3.539286415	0	NaN	1	1
329	centromere	21.60758377	12.31319959	5.300855105	0.086174944	0.750322464	0.620626515	0.956912528
330	nucleolar	9.900554599	3.07896423	3.431836017	0	NaN	1	1
331	nucleolar	10.32098909	2.755012218	3.148560895	0	NaN	1	1
332	centromere	22.71686523	11.74945066	5.05331039	0.082115875	0.765781998	0.646052372	0.95906963
333	homogeneous	52.03221649	24.16648275	6.125001229	0.057024354	0.960132527	0.299652053	0.971487823
334	nucleolar	18.102886	10.65027874	4.538833888	0.018605193	0.918920988	0.758907571	0.990697403
335	coarse_speckled	17.59903382	2.826265203	3.510665754	0	NaN	1	1
336	centromere	15.35272537	4.012341108	3.872729939	0	NaN	1	1
337	fine_speckled	35.33702882	12.83478007	5.405311861	0.031979492	0.930976105	0.505447403	0.984010254
338	centromere	10.38682389	2.402263746	2.819154294	0	NaN	1	1
339	fine_speckled	23.30914286	6.726755538	4.65564313	0.026100946	0.87588135	0.764597642	0.986949527
340	homogeneous	33.61892202	7.824097497	4.367336303	0.028642023	0.925041657	0.589495646	0.985678989
341	fine_speckled	25.53592503	6.157272568	4.533343735	0.055851077	0.810627462	0.652777292	0.972074462
342	centromere	19.60436747	9.681676024	4.520516053	0.056059259	0.75678192	0.745447028	0.97197037
343	homogeneous	12.98572066	3.301859049	3.458354577	0.00114345	0.374427752	0.997032876	0.999428275
344	nucleolar	19.80336538	14.27148293	4.872000978	0.03540165	0.904585574	0.727467521	0.982353973
345	homogeneous	55.8790493	23.43312713	6.063908307	0.057277367	0.956890014	0.347621071	0.971361317
346	coarse_speckled	26.74776828	7.765329925	4.852915074	0.099552367	0.753457854	0.507053054	0.950223816
347	nucleolar	10.70186916	3.245663305	3.50308289	0	NaN	1	1
348	centromere	22.03586066	14.03920075	5.139388095	0.054007044	0.870379692	0.62374	0.972996478
349	cytoplasmatic	23.50101382	5.51137106	4.059266422	0.046412977	0.793375181	0.731223398	0.976793512
350	homogeneous	36.9077381	8.835238517	4.689911894	0.035652602	0.89382111	0.628715252	0.982173699
351	centromere	16.23736325	8.511253422	4.36906376	0.04557603	0.67709454	0.833277622	0.977259253

352	cytoplasmatic	35.49555985	20.39789969	5.712353711	0.086713516	0.921710288	0.379347586	0.956741793
353	nucleolar	13.1099209	3.92293663	3.805266651	0	NaN	1	1
354	coarse_speckled	39.71415525	12.67153154	5.534023747	0.058317058	0.870273063	0.526495626	0.970841471
355	coarse_speckled	19.35001854	4.1541191	4.042512382	0.002703285	0.531253133	0.991539199	0.998648357
356	homogeneous	13.49847228	3.102114583	3.484132166	0	NaN	1	1
357	fine_speckled	37.75453622	11.13019457	5.35109849	0.030332365	0.922765509	0.577347713	0.984833818
358	centromere	18.17643541	8.849773981	4.619528251	0.050014528	0.714970585	0.79409693	0.975043821
359	homogeneous	14.70545775	3.820875524	3.768139595	0	NaN	1	1
360	cytoplasmatic	27.81681187	6.744220247	4.587106051	0.041676751	0.900853091	0.539822017	0.979161624
361	homogeneous	38.18809524	8.975078345	4.86695322	0.036372515	0.892273876	0.626630994	0.981813742
362	coarse_speckled	37.97123408	11.23722626	5.394215796	0.086996539	0.787147244	0.5292699	0.95650173
363	fine_speckled	19.15633423	4.683829537	4.106242777	0	NaN	1	1
364	homogeneous	37.06182352	9.227443765	4.623940988	0.031541011	0.914737629	0.598628243	0.984229494
365	fine_speckled	22.27689873	4.98101201	4.246455072	0.009364523	0.7216513	0.957123379	0.995317738
366	fine_speckled	48.00565571	17.42748211	5.880961533	0.086326826	0.902368733	0.34620718	0.956836587
367	fine_speckled	19.5935518	4.287864732	4.029679231	0	NaN	1	1
368	nucleolar	18.70970525	14.23739165	4.669059585	0.034100641	0.898665814	0.752560889	0.982949679
369	centromere	10.38397834	2.922467052	3.344660941	0	NaN	1	1
370	homogeneous	33.27325261	11.43562594	4.865461351	0.027406805	0.942380893	0.497464552	0.986296597
371	centromere	11.26810616	2.571152243	2.92905484	0.000572165	0.374713786	0.998514123	0.999713918
372	centromere	16.62139467	8.653122745	4.397976003	0.043751366	0.680783042	0.849694353	0.978249395
373	cytoplasmatic	37.89896907	19.08048431	5.728007709	0.104699861	0.901628803	0.354611118	0.94772256
374	centromere	18.16637194	10.48542636	4.837483059	0.062136006	0.706869296	0.760281038	0.968982334
375	coarse_speckled	37.27494505	13.6568266	5.563690669	0.063125846	0.873065957	0.482066383	0.968437077
376	centromere	10.54436782	2.535275306	2.769987526	0	NaN	1	1

377	homogeneous	15.2304613	3.251878456	3.376104341	0	NaN	1	1
378	nucleolar	13.71876425	4.186551529	3.937266929	0	NaN	1	1
379	cytoplasmatic	23.49928024	4.135906042	3.95092553	0.018709037	0.760748476	0.903429906	0.990645482
380	homogeneous	36.5974026	12.77199309	5.092708419	0.027866287	0.933188966	0.556795274	0.986066857
381	nucleolar	20.04389443	11.13428153	4.669289757	0.02178338	0.914903211	0.750635144	0.98910831
382	homogeneous	11.47264368	2.514718439	3.185377636	0	NaN	1	1
383	homogeneous	36.82623008	10.18798111	4.755678241	0.032861175	0.916659532	0.573217437	0.983569413
384	centromere	17.46768337	10.6033291	4.715479527	0.063164955	0.70829783	0.756154937	0.968479793
385	coarse_speckled	44.23831933	15.39565086	5.776924167	0.091586381	0.857823356	0.43275294	0.95420681
386	cytoplasmatic	26.52270621	5.201555254	4.20055334	0.095234035	0.714057174	0.581085312	0.952382983
387	centromere	15.60998811	9.380441936	4.387880626	0.050999142	0.674334114	0.827726824	0.974770327
388	centromere	11.80115582	3.568825803	3.581058967	0	NaN	1	1
389	nucleolar	19.94381313	12.6669196	4.936265662	0.02745877	0.913932649	0.697875515	0.986270615
390	centromere	26.10144566	13.50888893	5.320207412	0.105466122	0.786242426	0.531731631	0.947352717
391	homogeneous	66.66277453	24.09349661	6.267126051	0.06563268	0.947796278	0.350122185	0.96718366
392	cytoplasmatic	24.0185068	5.386069615	4.289597226	0.04576765	0.684165019	0.811454826	0.977116175
393	nucleolar	13.62180253	4.02121367	3.676701551	0	NaN	1	1
394	nucleolar	19.73585795	10.82499028	4.488482878	0.029098029	0.887183409	0.728601027	0.985450986
395	centromere	12.72136512	3.889443976	3.77269099	0	NaN	1	1
396	cytoplasmatic	21.10444331	4.234847159	3.817085451	0.006265393	0.451778184	0.98234691	0.996867304
397	centromere	12.35799874	2.324465273	3.174458426	0	NaN	1	1
398	centromere	14.2709465	3.031988985	3.568556459	0	NaN	1	1
399	fine_speckled	35.16648993	11.45171606	5.22369497	0.035021251	0.922298089	0.515107952	0.982489375
400	homogeneous	11.05209098	2.633665948	3.236399215	0	NaN	1	1
401	homogeneous	30.40019682	6.585515599	4.357973391	0.068703795	0.85431199	0.464282087	0.965648103

402	coarse_speckled	20.00625958	3.992945953	3.950071073	0.006048089	0.386267278	0.988924486	0.997669984
403	centromere	10.92035556	2.542886743	2.953798995	0	NaN	1	1
404	homogeneous	12.53218391	2.974444469	3.304083605	0	NaN	1	1
405	nucleolar	13.45095694	4.02140069	3.839153881	0	NaN	1	1
406	fine_speckled	25.33400402	6.916072661	4.632977135	0.052067323	0.838930735	0.627867669	0.973966339
407	cytoplasmatic	23.92455185	4.253655695	3.915075191	0.028646985	0.607082108	0.899308744	0.985676507
408	nucleolar	17.81141975	10.94445386	4.635401815	0.027588094	0.87859118	0.753201996	0.986205953
409	centromere	11.21781055	2.467299768	2.892175368	0	NaN	1	1
410	cytoplasmatic	21.55460365	5.929697101	3.9983412	0.038941072	0.752739865	0.80518474	0.980529464
411	homogeneous	33.49545455	7.354720262	4.43638083	0.033161942	0.916966079	0.56809812	0.983419029
412	nucleolar	17.13157895	10.69593214	4.456838281	0.020254013	0.901611096	0.778101847	0.989872994
413	coarse_speckled	28.30055096	8.636741494	5.000127017	0.089965467	0.811799681	0.440593107	0.955017267
414	centromere	18.91817924	13.01649995	4.990707489	0.068651631	0.789780751	0.728386986	0.965819428
415	centromere	10.81704754	2.563066272	2.924526005	0	NaN	1	1
416	nucleolar	24.05488822	14.28108649	5.095623354	0.042195106	0.906623098	0.652802269	0.978902447
417	nucleolar	17.35406872	9.711899214	4.471705869	0.025035128	0.866320807	0.788525939	0.987482436
418	centromere	9.187229011	2.738923446	3.273875156	0	NaN	1	1
419	fine_speckled	15.36227709	3.755970711	3.771534755	0	NaN	1	1
420	centromere	10.07093621	2.81447415	3.367515515	0	NaN	1	1
421	fine_speckled	38.89506173	11.99102551	5.229567276	0.029987016	0.923817145	0.576643151	0.985006492
422	centromere	33.8483705	14.45394765	5.541264931	0.110006084	0.834142899	0.397632317	0.945469633
423	cytoplasmatic	25.45783543	11.52200912	4.887935499	0.052903848	0.864550972	0.623102271	0.973548076
424	fine_speckled	36.09030379	13.34910901	5.531312686	0.041874695	0.905126067	0.517893207	0.979062652
425	coarse_speckled	18.71999314	3.696831944	3.838344419	0.002712708	0.294095575	0.993454312	0.998643646
426	nucleolar	12.51755364	3.10443121	3.445932412	0	NaN	1	1

427	cytoplasmatic	20.92049931	4.534735567	3.712940781	0.017078256	0.57363172	0.943175133	0.991460872
428	centromere	8.772821382	2.486136084	3.116114629	0	NaN	1	1
429	coarse_speckled	18.75072644	2.932838367	3.562674749	0	NaN	1	1
430	nucleolar	12.07676923	3.152109429	3.419180022	0	NaN	1	1
431	cytoplasmatic	23.18788927	6.113416266	4.2405185	0.056107147	0.715956845	0.752150335	0.972414385
432	centromere	21.13126362	10.26525002	4.853208696	0.064928032	0.738733496	0.703862163	0.967535984
433	coarse_speckled	28.49275362	7.558908084	4.807093601	0.082330286	0.828268881	0.445323761	0.958834857
434	cytoplasmatic	18.91600112	3.942326895	3.43422821	0.008896254	0.531813937	0.972188028	0.995551873
435	fine_speckled	37.40602564	13.40546589	5.545101199	0.032772205	0.926610385	0.52529735	0.983613898
436	centromere	16.59868545	7.286239911	4.47537559	0.043471079	0.598178606	0.850393916	0.978264461
437	coarse_speckled	47.46904861	18.9902973	5.967025635	0.111307454	0.892600307	0.297903761	0.944346273
438	coarse_speckled	19.01402732	5.058690688	4.286481208	0.009714088	0.551123711	0.96876179	0.995142956
439	cytoplasmatic	22.62934923	2.917557847	3.50544669	0.002900482	0.518815632	0.991084411	0.998549759
440	nucleolar	10.98897059	2.653036113	3.089000975	0	NaN	1	1
441	fine_speckled	37.64141414	8.257509175	4.959548319	0.031094125	0.906554669	0.636868559	0.984452937
442	fine_speckled	24.38792074	3.618792772	3.8005987	0.012359869	0.550750169	0.960331634	0.993820065
443	centromere	10.72374461	2.440880179	2.79223425	0	NaN	1	1
444	homogeneous	38.33375252	9.75439408	5.116890562	0.036502293	0.895873288	0.613337414	0.981748854
445	coarse_speckled	20.27462765	4.352475076	4.073951464	0.009244118	0.555455439	0.970060886	0.995377941
446	fine_speckled	22.17059484	6.380379974	4.435295256	0.015296973	0.544157791	0.959104605	0.993526838
447	fine_speckled	43.60373382	12.5152461	5.361841683	0.032769163	0.896168124	0.661698051	0.983615419
448	fine_speckled	41.16901961	14.06363752	5.640766899	0.047115377	0.893998883	0.538831507	0.976442311
449	centromere	16.985688	5.024296757	4.18004503	0	NaN	1	1
450	nucleolar	19.0745614	10.48902586	4.705383897	0.023252135	0.90475181	0.733452751	0.988373933
451	fine_speckled	39.83795929	13.09416472	5.506666035	0.033756103	0.91455035	0.575130859	0.983121949

452	homogeneous	37.51341223	9.204956636	4.842447766	0.026983823	0.917599199	0.645416098	0.986508088
453	coarse_speckled	36.83800682	12.3906817	5.428328477	0.052562551	0.87784576	0.528109912	0.973718724
454	homogeneous	33.74939875	6.035754137	4.49349933	0.050523849	0.863301009	0.581801959	0.974738076
455	fine_speckled	40.17218417	13.97316426	5.487315608	0.038313449	0.911328994	0.534848199	0.980843275
456	centromere	20.02936508	10.05842877	4.811085215	0.072488879	0.688950383	0.717336889	0.963755561
457	cytoplasmatic	39.18541559	17.53506656	5.63733583	0.113038439	0.881109757	0.333800559	0.943493226
458	homogeneous	36.50603715	7.472121531	4.76578782	0.032093688	0.89278117	0.669128396	0.983953156
459	coarse_speckled	47.3973035	18.39317586	5.903210638	0.108969578	0.888191415	0.314215028	0.945515211
460	centromere	9.230710853	2.143131843	2.998783856	0	NaN	1	1
461	homogeneous	42.66590721	10.01972478	5.066106533	0.021028398	0.911996361	0.739821429	0.989485801
462	fine_speckled	15.32903795	2.736377187	3.35819301	0	NaN	1	1
463	homogeneous	67.28441944	28.48557533	6.417741486	0.076404203	0.960346726	0.251468013	0.961797898
464	homogeneous	44.84430177	21.13526191	6.069239335	0.050089111	0.952533038	0.334578039	0.974955445
465	nucleolar	11.49459061	2.723254457	3.190331586	0	NaN	1	1
466	coarse_speckled	19.0821256	3.588642049	3.837202278	0.001077676	0.299460747	0.997386526	0.999461162
467	fine_speckled	15.04390837	4.115370809	3.938900877	0	NaN	1	1
468	coarse_speckled	19.41898914	4.018109986	4.004539077	0.0016061	0.374195917	0.995832229	0.99919695
469	homogeneous	39.50704562	9.284797391	4.893652578	0.021719726	0.933770993	0.650373604	0.989140137
470	fine_speckled	22.43631485	4.988712041	4.193942262	0.013160811	0.666011835	0.9476563	0.993419594
471	cytoplasmatic	41.58629149	24.51762465	5.946172092	0.124784134	0.919704127	0.313864097	0.938048275
472	fine_speckled	39.92878651	14.71443436	5.611204468	0.040946856	0.910960614	0.525338204	0.979526572
473	homogeneous	51.20232804	29.28504029	6.417039073	0.082206377	0.956540293	0.255625938	0.958896812
474	centromere	28.07518116	14.06221109	5.405553434	0.111501894	0.80541521	0.470127373	0.94435335
475	centromere	10.95503962	2.464530157	3.004072725	0	NaN	1	1
476	nucleolar	17.04493587	4.830909164	4.103111731	0.004535343	0.685987316	0.98105135	0.997732329

477	fine_speckled	15.2870674	3.197044482	3.502952082	0	NaN	1	1
478	centromere	11.512123	2.964724489	3.135003792	0	NaN	1	1
479	cytoplasmatic	29.82097801	14.73326302	5.139229514	0.064911777	0.901459453	0.51189388	0.967557637
480	homogeneous	31.37021696	7.732202823	4.806502992	0.057877279	0.882371751	0.453577682	0.971061361
481	homogeneous	44.85930736	10.14203685	5.182295909	0.033065871	0.860647798	0.742027461	0.983467064
482	cytoplasmatic	36.03362971	18.74562503	5.33640708	0.089568473	0.914197232	0.408671088	0.955215763
483	centromere	12.85336368	4.415796968	3.866198989	0	NaN	1	1
484	fine_speckled	36.16778885	10.68476328	5.072513512	0.033568972	0.914745243	0.573280572	0.983215514
485	centromere	22.84424655	13.41434495	5.307152797	0.083929082	0.804374253	0.620898804	0.959583393
486	centromere	10.95473058	2.318110388	2.922525481	0	NaN	1	1
487	fine_speckled	13.14522692	2.669785652	3.100693038	0	NaN	1	1
488	centromere	24.02325211	13.52439659	5.022631111	0.079808746	0.825802594	0.603959158	0.960421826
489	coarse_speckled	31.73777778	9.707816717	5.128162327	0.066518789	0.86511794	0.444711755	0.966740606
490	centromere	13.19539911	2.974562687	3.498223466	0	NaN	1	1
491	nucleolar	18.37406082	10.70327888	4.614333383	0.028147476	0.878942927	0.741623366	0.985926262
492	fine_speckled	15.4828365	3.506840249	3.629471964	0	NaN	1	1
493	centromere	10.90159016	2.940483933	3.442851052	0	NaN	1	1
494	centromere	10.28962435	3.017762108	3.030666288	0.002846831	0.374643943	0.998152093	0.999525528
495	centromere	10.03954616	2.311550024	2.746214726	0	NaN	1	1
496	centromere	11.49503438	3.979165035	3.612242789	0	NaN	1	1
497	centromere	13.79336043	4.096372081	3.886065848	0.000864878	0.374567261	0.997754865	0.999567561
498	coarse_speckled	39.3975417	14.15367986	5.517190436	0.062236524	0.883683871	0.473810449	0.968881738
499	nucleolar	16.10550796	11.71781829	4.590588757	0.022922104	0.900873264	0.746558056	0.988538948
500	coarse_speckled	49.90669516	19.85450689	6.013870268	0.130136784	0.875856557	0.289418685	0.934931608
501	coarse_speckled	20.20534665	3.678159374	3.880725103	0.001497185	0.165917401	0.996711315	0.999251408

502	centromere	18.9506095	11.28330115	4.66036635	0.072772094	0.730926945	0.732229437	0.964332163
503	homogeneous	13.42687179	2.968189984	3.232400699	0	NaN	1	1
504	fine_speckled	34.64870382	11.81162907	5.291319559	0.031788997	0.93001921	0.514670425	0.984105502
505	centromere	10.55016447	3.505750486	3.470405716	0	NaN	1	1
506	homogeneous	12.44130571	2.792768807	3.107041921	0	NaN	1	1
507	centromere	13.14339043	3.612500141	3.5933506	0	NaN	1	1
508	fine_speckled	13.31545455	1.996557496	2.87395638	0	NaN	1	1
509	coarse_speckled	19.48380537	4.123765188	4.039124876	0.002219585	0.373888233	0.994241767	0.998890207
510	nucleolar	18.46957506	11.9825785	4.487665942	0.025599454	0.899405228	0.741847446	0.987200273
511	homogeneous	36.89925926	10.22587283	4.805352272	0.030991625	0.92090208	0.577358073	0.984504187
512	homogeneous	36.86943886	8.177751247	4.808522416	0.035881199	0.89199506	0.632499267	0.982059401
513	homogeneous	14.07342657	3.237512962	3.4669326	0	NaN	1	1
514	homogeneous	59.02619431	24.20839843	6.07798689	0.050714879	0.961622112	0.361101708	0.97464256
515	nucleolar	9.995655806	2.606997956	3.277815349	0	NaN	1	1
516	nucleolar	12.82326389	3.856872165	3.76272571	0	NaN	1	1
517	coarse_speckled	45.00785773	17.45743058	5.839577014	0.108440189	0.870208386	0.351260415	0.945779905
518	nucleolar	11.1743567	2.745801237	3.26296702	0	NaN	1	1
519	centromere	11.02680412	2.816927435	2.826332537	0	NaN	1	1
520	homogeneous	57.00382592	21.77223822	6.016873778	0.06092215	0.953684178	0.342214647	0.969538925
521	centromere	10.96713615	2.267317894	2.923020997	0	NaN	1	1
522	nucleolar	19.72270672	10.71863684	4.706823107	0.024104799	0.903687835	0.726292906	0.9879476
523	centromere	13.39578215	4.734048268	4.081077258	0	NaN	1	1
524	fine_speckled	30.21288462	12.63217902	5.366659214	0.026464986	0.946993229	0.474954656	0.986767507
525	fine_speckled	31.03797468	9.468966354	5.14816105	0.043380116	0.913184755	0.458888879	0.978309942
526	centromere	13.49366768	8.244918472	4.27459905	0.033203622	0.669512188	0.880779062	0.983441372

527	nucleolar	21.6467413	13.43958459	4.801953384	0.041828701	0.880091367	0.67761679	0.97908565
528	homogeneous	38.07917151	10.03811342	4.999891914	0.037309647	0.901663954	0.584119691	0.981345176
529	fine_speckled	13.47667262	3.271125179	3.548916717	0	NaN	1	1
530	centromere	16.06071289	7.888165164	4.496087428	0.044009071	0.608593062	0.850190221	0.977995465
531	coarse_speckled	34.49857923	10.58294059	5.316583084	0.091197952	0.820150442	0.434653215	0.9555953
532	cytoplasmatic	25.26301654	13.20943507	5.31099495	0.048251071	0.886241529	0.591221194	0.975874464
533	homogeneous	42.76809211	14.88623715	5.686285536	0.090396055	0.857162693	0.432329251	0.954801973
534	cytoplasmatic	33.90626338	18.73311	5.452573722	0.089353695	0.909694876	0.438997329	0.955619231
535	centromere	10.52710843	2.331864355	2.781507733	0	NaN	1	1
536	fine_speckled	13.55670363	2.882771406	3.256703194	0	NaN	1	1
537	homogeneous	17.08605442	5.246607927	4.187546444	0	NaN	1	1
538	centromere	10.63274911	2.278026096	2.909595445	0	NaN	1	1
539	homogeneous	12.48397436	2.072493188	2.880760296	0	NaN	1	1
540	centromere	16.74902138	10.38580149	4.625315754	0.050130006	0.745530203	0.78197139	0.974986437
541	cytoplasmatic	22.82671958	3.039274275	3.596484835	0.002129318	0.248933828	0.995040609	0.998935341
542	coarse_speckled	22.89013283	5.996224961	4.473158647	0.045103076	0.635933586	0.833205564	0.977448462
543	homogeneous	13.27481161	3.371221376	3.449138855	0	NaN	1	1
544	cytoplasmatic	31.23971572	10.11873874	5.013827241	0.084998762	0.832641413	0.440897427	0.957500619
545	homogeneous	49.91933638	13.62406425	5.637909096	0.070893033	0.862853449	0.52902983	0.964553484
546	coarse_speckled	18.73519164	3.960225991	3.99003225	0.00137364	0.392169545	0.996370989	0.99931318
547	centromere	15.82032164	7.755137115	4.551319566	0.029482942	0.70497852	0.879469309	0.985258529
548	coarse_speckled	34.2767094	9.766133252	5.162803736	0.089435421	0.804170602	0.461738019	0.95528229
549	centromere	9.023524721	2.100620622	2.957279398	0	NaN	1	1
550	centromere	13.1921944	3.25513168	3.476768327	0	NaN	1	1
551	coarse_speckled	33.84466218	11.23161615	5.320330647	0.070259708	0.850122577	0.466908767	0.964870146

552	homogeneous	31.67958861	7.977021983	4.561830781	0.036563587	0.921167093	0.500631835	0.981718206
553	cytoplasmatic	21.17224646	5.040861272	3.889101836	0.033011867	0.61401657	0.882597756	0.983494067
554	centromere	11.43146706	3.161627714	3.265879667	0	NaN	1	1
555	homogeneous	36.99408284	9.395148268	4.671993017	0.026378384	0.93304353	0.579850756	0.986810808
556	homogeneous	60.43047523	18.0055458	5.956085768	0.045916318	0.94673739	0.40994185	0.977041841
557	centromere	20.76008065	12.76934162	4.845646905	0.081431036	0.771027036	0.676951305	0.959911869
558	centromere	21.34089347	12.76714983	5.106559206	0.066818406	0.808758769	0.651010865	0.966590797
559	centromere	10.32910401	2.159674591	2.828435855	0	NaN	1	1
560	coarse_speckled	47.44251208	16.52984935	5.897999958	0.108854635	0.856413204	0.37761373	0.945572683
561	homogeneous	34.14876899	8.004574845	4.490803658	0.034287405	0.912662185	0.57353957	0.982856297
562	coarse_speckled	35.80060606	9.917727822	5.188704826	0.053060827	0.878520429	0.513475074	0.973469587
563	fine_speckled	37.86529412	11.47144837	5.215456349	0.035590341	0.908977183	0.573894767	0.982204829
564	centromere	10.8543546	3.721538248	3.514446092	0	NaN	1	1
565	fine_speckled	37.88447927	13.26583414	5.45589824	0.029203903	0.93032495	0.55237012	0.985398049
566	nucleolar	18.66697531	10.79378707	4.51415255	0.036126497	0.858888104	0.756382213	0.981936752
567	coarse_speckled	17.91026405	3.164519827	3.667762825	0	NaN	1	1
568	cytoplasmatic	28.28344671	11.56390627	5.115468373	0.073103927	0.850870719	0.502131912	0.963543655
569	coarse_speckled	16.9106153	3.053038814	3.622412673	0	NaN	1	1
570	fine_speckled	12.55048288	2.683950274	3.204266583	0	NaN	1	1
571	nucleolar	11.35728814	4.535648043	3.901981953	0	NaN	1	1
572	cytoplasmatic	36.7242061	16.57439429	5.465433068	0.097092334	0.891700627	0.373234764	0.951474764
573	centromere	20.70228466	11.30166814	4.628801202	0.059014505	0.800813596	0.739445254	0.971120282
574	centromere	17.75146277	9.156894367	4.497478444	0.058960914	0.664083877	0.790881181	0.970610283
575	fine_speckled	39.21934901	14.37815087	5.546993017	0.041750615	0.906889741	0.519704772	0.979124693
576	coarse_speckled	41.51446281	15.90518757	5.717949398	0.076614667	0.877959904	0.43506706	0.961692666

577	nucleolar	17.33876712	11.73473321	4.699592848	0.027781727	0.893006541	0.76065669	0.986109136
578	centromere	9.145466406	2.802655147	3.290724786	0	NaN	1	1
579	cytoplasmatic	32.28737758	17.75952795	5.394243852	0.093939138	0.892700112	0.429562535	0.953262539
580	homogeneous	36.2512071	8.354434988	4.563789437	0.036843141	0.897890135	0.603119121	0.981578429
581	coarse_speckled	24.24891041	7.184590357	4.781732515	0.062051299	0.784121785	0.65472617	0.968974351
582	homogeneous	15.26948519	5.460539045	4.131648159	0	NaN	1	1
583	fine_speckled	17.35250464	3.619105733	3.783118501	0	NaN	1	1
584	nucleolar	19.83968087	12.67866747	4.747080216	0.036004982	0.887889245	0.739600632	0.981997509
585	homogeneous	33.62318841	5.535903903	4.335930954	0.065717802	0.832395603	0.549872662	0.968076532
586	cytoplasmatic	34.43868284	17.20365022	5.607483981	0.082289718	0.905557265	0.406407928	0.958855141
587	centromere	13.23037348	4.239056213	3.805934814	0	NaN	1	1
588	homogeneous	62.3505618	27.63478379	6.376077711	0.070494097	0.961281383	0.266303472	0.964752951
589	centromere	13.62027972	4.021289685	3.860138186	0	NaN	1	1
590	coarse_speckled	29.21768576	8.550016819	4.933754098	0.094409146	0.8105465	0.416436168	0.952795427
591	cytoplasmatic	23.0536829	3.546283533	3.801873691	0.002789736	0.403686599	0.992542214	0.998605132
592	centromere	20.96271478	12.27227982	4.769663953	0.062509298	0.81348537	0.70944534	0.968745351
593	centromere	23.31400966	15.11158634	5.242688145	0.098362782	0.806252963	0.61576913	0.952590373
594	nucleolar	19.27159023	13.65712794	4.794119728	0.034844134	0.887432132	0.734267548	0.982577933
595	coarse_speckled	46.52476959	19.13255593	5.917175555	0.124279888	0.880151584	0.29443707	0.937860056
596	homogeneous	65.07681756	25.34711247	6.227844733	0.072314333	0.944564813	0.326740815	0.963842834
597	fine_speckled	31.58149711	12.61234137	5.502882974	0.032234066	0.936040817	0.468882314	0.983882967
598	centromere	11.40696118	2.491119431	2.841710999	0	NaN	1	1
599	fine_speckled	31.93453843	10.49933407	5.203433603	0.038807049	0.920717332	0.47309195	0.980596475
600	fine_speckled	25.12190635	6.728109527	4.683652603	0.043811762	0.857526639	0.651008566	0.978094119
601	coarse_speckled	19.64672619	4.920824652	4.212837843	0.008420617	0.78547637	0.952437563	0.995789691

602	coarse_speckled	40.67014342	13.38087895	5.572896849	0.079531447	0.855405288	0.462327731	0.960234277
603	cytoplasmatic	30.55521768	13.32600168	5.186140657	0.072015804	0.877016164	0.475740756	0.963992098
604	cytoplasmatic	27.1322766	9.131937468	4.704738288	0.046568191	0.898189726	0.542333314	0.977060025
605	homogeneous	31.48400298	6.501729634	4.454519789	0.060640343	0.86983644	0.477008202	0.969679828
606	cytoplasmatic	30.39714362	13.53894573	5.178569153	0.069117032	0.882481136	0.487785968	0.965441484
607	centromere	11.98227848	2.603697299	3.199293916	0	NaN	1	1
608	cytoplasmatic	24.67081926	11.48396822	4.642517052	0.040935959	0.89334409	0.660404178	0.979537998
609	coarse_speckled	19.23445239	4.150745923	4.013038743	0.003184825	0.148404598	0.993087372	0.998407587
610	coarse_speckled	43.02479167	14.57466745	5.70662102	0.09643518	0.838729446	0.44562925	0.95178241
611	coarse_speckled	17.64096728	3.347043963	3.734202047	0.000942975	0.457861435	0.997321234	0.999528512
612	homogeneous	12.46907692	2.598743422	3.052461133	0	NaN	1	1
613	coarse_speckled	38.08823529	12.38845205	5.52687223	0.069739985	0.849108578	0.507296216	0.965130008
614	homogeneous	14.79029734	4.461009995	3.817967331	0	NaN	1	1
615	coarse_speckled	19.08116883	3.275312177	3.725170949	0	NaN	1	1
616	centromere	22.00097007	14.33209229	5.123596552	0.080920232	0.819678244	0.650463403	0.960106964
617	homogeneous	19.43153301	6.803641791	4.29581287	0	NaN	1	1
618	centromere	10.71108925	2.126026264	2.606654893	0	NaN	1	1
619	coarse_speckled	55.26656234	21.87928825	6.295443051	0.140265317	0.8861433	0.259781149	0.929867342
620	homogeneous	38.85903668	9.991687876	5.131775688	0.032178304	0.911933657	0.602687366	0.983910848
621	coarse_speckled	55.77391058	20.15233771	6.260026299	0.126513256	0.875336706	0.298961966	0.936743372

A3: Features extracted from Training Set

A4: Classification Results for Training Set (* Classification Yes/No)

#	Pattern	TRUE	#	Pattern	TRUE	#	Pattern	TRUE	#	Pattern	TRUE	#	Pattern	TRUE
1	Homogeneous	Yes	1	Fine-Speckled	No	1	Coarse-Speckled	Yes	1	Centromere	Yes	1	Nucleolar	No
2	Homogeneous	Yes	2	Fine-Speckled	Yes	2	Coarse-Speckled	No	2	Centromere	Yes	2	Nucleolar	Yes
3	Homogeneous	No	3	Fine-Speckled	Yes	3	Coarse-Speckled	No	3	Centromere	No	3	Nucleolar	Yes
4	Homogeneous	No	4	Fine-Speckled	Yes	4	Coarse-Speckled	Yes	4	Centromere	Yes	4	Nucleolar	Yes
5	Homogeneous	Yes	5	Fine-Speckled	No	5	Coarse-Speckled	Yes	5	Centromere	Yes	5	Nucleolar	No
6	Homogeneous	Yes	6	Fine-Speckled	Yes	6	Coarse-Speckled	Yes	6	Centromere	No	6	Nucleolar	Yes
7	Homogeneous	Yes	7	Fine-Speckled	No	7	Coarse-Speckled	No	7	Centromere	No	7	Nucleolar	Yes
8	Homogeneous	Yes	8	Fine-Speckled	Yes	8	Coarse-Speckled	Yes	8	Centromere	No	8	Nucleolar	Yes
9	Homogeneous	Yes	9	Fine-Speckled	Yes	9	Coarse-Speckled	Yes	9	Centromere	Yes	9	Nucleolar	No
10	Homogeneous	No	10	Fine-Speckled	Yes	10	Coarse-Speckled	Yes	10	Centromere	Yes	10	Nucleolar	No
11	Homogeneous	Yes	11	Fine-Speckled	No	11	Coarse-Speckled	No	11	Centromere	Yes	11	Nucleolar	Yes
12	Homogeneous	Yes	12	Fine-Speckled	Yes	12	Coarse-Speckled	No	12	Centromere	Yes	12	Nucleolar	Yes
13	Homogeneous	Yes	13	Fine-Speckled	Yes	13	Coarse-Speckled	Yes	13	Centromere	No	13	Nucleolar	Yes
14	Homogeneous	No	14	Fine-Speckled	Yes	14	Coarse-Speckled	Yes	14	Centromere	No	14	Nucleolar	Yes
15	Homogeneous	No	15	Fine-Speckled	Yes	15	Coarse-Speckled	No	15	Centromere	Yes	15	Nucleolar	No
16	Homogeneous	Yes	16	Fine-Speckled	No	16	Coarse-Speckled	Yes	16	Centromere	Yes	16	Nucleolar	Yes
17	Homogeneous	Yes	17	Fine-Speckled	Yes	17	Coarse-Speckled	Yes	17	Centromere	Yes	17	Nucleolar	No
18	Homogeneous	Yes	18	Fine-Speckled	No	18	Coarse-Speckled	Yes	18	Centromere	Yes	18	Nucleolar	Yes
19	Homogeneous	Yes	19	Fine-Speckled	No	19	Coarse-Speckled	Yes	19	Centromere	Yes	19	Nucleolar	Yes
20	Homogeneous	Yes	20	Fine-Speckled	Yes	20	Coarse-Speckled	No	20	Centromere	No	20	Nucleolar	No
21	Homogeneous	No	21	Fine-Speckled	Yes	21	Coarse-Speckled	No	21	Centromere	Yes	21	Nucleolar	Yes
22	Homogeneous	No	22	Fine-Speckled	Yes	22	Coarse-Speckled	Yes	22	Centromere	No	22	Nucleolar	Yes
23	Homogeneous	Yes	23	Fine-Speckled	Yes	23	Coarse-Speckled	Yes	23	Centromere	No	23	Nucleolar	No
24	Homogeneous	No	24	Fine-Speckled	No	24	Coarse-Speckled	No	24	Centromere	Yes	24	Nucleolar	Yes

25	Homogeneous	Yes	**25**	Fine-Speckled	Yes	**25**	Coarse-Speckled	Yes	**25**	Centromere	Yes	**25**	Nucleolar	Yes
26	Homogeneous	No	**26**	Fine-Speckled	Yes	**26**	Coarse-Speckled	Yes	**26**	Centromere	Yes	**26**	Nucleolar	Yes
27	Homogeneous	Yes	**27**	Fine-Speckled	No	**27**	Coarse-Speckled	Yes	**27**	Centromere	Yes	**27**	Nucleolar	Yes
28	Homogeneous	Yes	**28**	Fine-Speckled	Yes	**28**	Coarse-Speckled	Yes	**28**	Centromere	Yes	**28**	Nucleolar	Yes
29	Homogeneous	Yes	**29**	Fine-Speckled	Yes	**29**	Coarse-Speckled	No	**29**	Centromere	No	**29**	Nucleolar	Yes
30	Homogeneous	No	**30**	Fine-Speckled	Yes	**30**	Coarse-Speckled	No	**30**	Centromere	Yes	**30**	Nucleolar	No
31	Homogeneous	No	**31**	Fine-Speckled	No	**31**	Coarse-Speckled	Yes	**31**	Centromere	Yes	**31**	Nucleolar	Yes
32	Homogeneous	Yes	**32**	Fine-Speckled	No	**32**	Coarse-Speckled	No	**32**	Centromere	Yes	**32**	Nucleolar	Yes
33	Homogeneous	Yes	**33**	Fine-Speckled	No	**33**	Coarse-Speckled	Yes	**33**	Centromere	No	**33**	Nucleolar	Yes
34	Homogeneous	Yes	**34**	Fine-Speckled	Yes	**34**	Coarse-Speckled	Yes	**34**	Centromere	Yes	**34**	Nucleolar	Yes
35	Homogeneous	Yes	**35**	Fine-Speckled	Yes	**35**	Coarse-Speckled	No	**35**	Centromere	Yes	**35**	Nucleolar	No
36	Homogeneous	No	**36**	Fine-Speckled	No	**36**	Coarse-Speckled	No	**36**	Centromere	Yes	**36**	Nucleolar	No
37	Homogeneous	Yes	**37**	Fine-Speckled	Yes	**37**	Coarse-Speckled	Yes	**37**	Centromere	No	**37**	Nucleolar	Yes
38	Homogeneous	No	**38**	Fine-Speckled	Yes	**38**	Coarse-Speckled	Yes	**38**	Centromere	No	**38**	Nucleolar	Yes
39	Homogeneous	No	**39**	Fine-Speckled	Yes	**39**	Coarse-Speckled	Yes	**39**	Centromere	Yes	**39**	Nucleolar	Yes
40	Homogeneous	Yes	**40**	Fine-Speckled	Yes	**40**	Coarse-Speckled	No	**40**	Centromere	Yes	**40**	Nucleolar	No
41	Homogeneous	Yes	**41**	Fine-Speckled	No	**41**	Coarse-Speckled	Yes	**41**	Centromere	Yes	**41**	Nucleolar	Yes
42	Homogeneous	Yes	**42**	Fine-Speckled	Yes	**42**	Coarse-Speckled	Yes	**42**	Centromere	No	**42**	Nucleolar	Yes
43	Homogeneous	Yes	**43**	Fine-Speckled	No	**43**	Coarse-Speckled	Yes	**43**	Centromere	Yes	**43**	Nucleolar	No
44	Homogeneous	Yes	**44**	Fine-Speckled	No	**44**	Coarse-Speckled	No	**44**	Centromere	Yes	**44**	Nucleolar	Yes
45	Homogeneous	No	**45**	Fine-Speckled	Yes	**45**	Coarse-Speckled	No	**45**	Centromere	Yes	**45**	Nucleolar	Yes
46	Homogeneous	Yes	**46**	Fine-Speckled	No s	**46**	Coarse-Speckled	No	**46**	Centromere	Yes	**46**	Nucleolar	No
47	Homogeneous	Yes	**47**	Fine-Speckled	No	**47**	Coarse-Speckled	Yes	**47**	Centromere	No	**47**	Nucleolar	No
48	Homogeneous	No	**48**	Fine-Speckled	Yes	**48**	Coarse-Speckled	Yes	**48**	Centromere	No	**48**	Nucleolar	Yes
49	Homogeneous	Yes	**49**	Fine-Speckled	Yes	**49**	Coarse-Speckled	No	**49**	Centromere	Yes	**49**	Nucleolar	Yes
50	Homogeneous	No	**50**	Fine-Speckled	Yes	**50**	Coarse-Speckled	Yes	**50**	Centromere	Yes	**50**	Nucleolar	Yes